Charcot-Marie-Tooth disease-linked protein SIMPLE functions with the ESCRT machinery in endosomal trafficking

Samuel M. Lee, Lih-Shen Chin, and Lian Li

Department of Pharmacology and Center for Neurodegenerative Disease, Emory University School of Medicine, Atlanta, GA 30322

Mutations in small integral membrane protein of lysosome/late endosome (SIMPLE) cause autosomal dominant, Charcot-Marie-Tooth disease (CMT) type 1C. The cellular function of SIMPLE is unknown and the pathogenic mechanism of SIMPLE mutations remains elusive. Here, we report that SIMPLE interacted and colocalized with endosomal sorting complex required for transport (ESCRT) components STAM1, Hrs, and TSG101 on early endosomes and functioned with the ESCRT machinery in the control of endosome-to-lysosome trafficking. Our analyses revealed that SIMPLE was required for efficient recruitment of ESCRT components to endosomal membranes and for regulating endosomal trafficking and signaling attenuation of ErbB receptors. We found that the ability of SIMPLE to regulate ErbB trafficking and signaling was impaired by CMT-linked SIMPLE mutations via a loss-of-function, dominant-negative mechanism, resulting in prolonged activation of ERK1/2 signaling. Our findings indicate a function of SIMPLE as a regulator of endosomal trafficking and provide evidence linking dysregulated endosomal trafficking to CMT pathogenesis.

Introduction

Charcot-Marie-Tooth disease (CMT) is the most common inherited neurological disorder affecting the peripheral nervous system (Martyn and Hughes, 1997; Parman, 2007). The molecular mechanisms underlying CMT pathogenesis remain unclear, and currently there is no effective treatment to stop the progression of this debilitating disease. Small integral membrane protein of lysosome/late endosome (SIMPLE), also known as lipopolysaccharide-induced TNF factor (LITAF), is a ubiquitously expressed, 161–amino acid protein of unknown function (Moriwaki et al., 2001; Street et al., 2003). Our recent study reveals that endogenous SIMPLE is an early endosomal membrane protein (Lee et al., 2011) rather than a lysosomal/late endosomal protein, as previously suggested (Moriwaki et al., 2001). To date, eight distinct point mutations in SIMPLE have been identified as the genetic defects for causing dominantly inherited CMT type 1C (CMT1C; Street et al., 2003; Campbell et al., 2004; Saifi et al., 2005; Latour et al., 2006; Gerding et al., 2009). Thus, elucidation of the cellular function of SIMPLE and the functional consequences of SIMPLE mutations is essential for a mechanistic understanding of CMT pathogenesis.

Endocytic trafficking is crucial to the function and survival of all eukaryotic cells. Cell surface receptors are endocytosed upon ligand binding and then targeted to the early endosome. Once they arrive at the early endosome, the endocytosed receptors are either recycled to the cell surface or sorted to intralumenal vesicles of multivesicular bodies for delivery to the lysosome for degradation (Katzmann et al., 2002). Ligand-induced lysosomal degradation of cell surface receptors is a major mechanism that attenuates signaling of activated receptors (Waterman and Yarden, 2001; Katzmann et al., 2002). Ample evidence indicates that the endosomal sorting complex required for transport (ESCRT) machinery, composed of ESCRT-0, -I, -II, and -III complexes, plays a central role in the endosomal sorting of internalized cell surface receptors to the lysosomal pathway (Roxrud et al., 2010; Henne et al., 2011). However, the

Correspondence to Lih-Shen Chin: chinl@pharm.emory.edu; or Lian Li: lianli@pharm.emory.edu

Abbreviations used in this paper: CMT, Charcot-Marie-Tooth disease; CMT1C, CMT type 1C; C-rich, cysteine-rich; EGFR, EGF receptor; ESCRT, endosomal sorting complex required for transport; NRG1, neuregulin-1; PI(3)P, phosphatidylinositol-3-phosphate; 3D-SIM, 3D structured illumination microscopy; SIMPLE, small integral membrane protein of lysosome/late endosome; TMD, transmembrane domain; TR-EGF, Texas red–conjugated EGF; WT, wild type.

The Rockefeller University Press $30.00
J. Cell Biol. Vol. 199 No. 5 799–816
www.jcb.org/cgi/doi/10.1083/jcb.201204137

molecular mechanisms that regulate ESCRT function and confer temporal and spatial control to the endosome-to-lysosome trafficking process remain poorly understood.

SIMPLE contains a PSAP tetrapeptide motif that is predicated to bind TSG101, a subunit of the ESCRT-I complex (Pornillos et al., 2002). Although SIMPLE has been shown to interact with TSG101 (Shirk et al., 2005), the functional significance of the SIMPLE–TSG101 interaction has not yet been examined, and the question of whether SIMPLE has a role in regulation of endosomal sorting and trafficking remains unexplored. SIMPLE also contains a cysteine-rich (C-rich) domain, which is hypothesized to be a putative RING finger domain with E3 ubiquitin-protein ligase activity (Moriwaki et al., 2001; Saifi et al., 2005), but whether or not SIMPLE has an E3 ligase function remains to be determined.

In this study, we investigated the biochemical function and cellular role of SIMPLE and assessed the functional consequences of CMT1C-linked SIMPLE mutations. Our results revealed that SIMPLE functions with the ESCRT machinery in the control of endosome-to-lysosome trafficking and signaling attenuation. Furthermore, we found that CMT1C-linked SIMPLE mutants are loss-of-function mutants that act in a dominant-negative manner to impair endosomal trafficking, leading to prolonged ERK1/2 signaling downstream of ErbB activation. Our findings provide novel insights into the mechanism of SIMPLE action in normal physiology and in CMT pathogenesis, and have important implications for understanding and treating peripheral neuropathy.

Results

SIMPLE interacts and colocalizes with STAM1, Hrs, and TSG101 on early endosomes

To gain insights into the cellular function of SIMPLE, we performed yeast two-hybrid screens for SIMPLE-binding proteins using full-length human SIMPLE as bait. A positive clone isolated from the screens encodes the N-terminal 315 amino acids of STAM1 (Fig. 1 A). We further examined the identified interaction by using an in vitro binding assay with purified recombinant proteins and found that SIMPLE interacted directly with STAM1 (Fig. 1 B). Coimmunoprecipitation analysis revealed that SIMPLE coprecipitated with STAM1 (Fig. 1 C), confirming the interaction of SIMPLE with STAM1 in transfected cells.

Because STAM1 forms ESCRT-0 complex with Hrs, we assessed the association of endogenous SIMPLE, STAM1, and Hrs in HeLa cells by coimmunoprecipitation analysis and found that endogenous SIMPLE interacted with both STAM1 and Hrs in cells (Fig. 1 D). We then performed in vitro binding assays and found that SIMPLE did not directly interact with Hrs, though it interacted with Hrs when STAM1 was present (Fig. S1 A). Furthermore, SIMPLE had no effect on the interaction of Hrs with STAM1 (Fig. S1 A), which indicates that SIMPLE and Hrs do not compete for STAM1 binding. Together, these results indicate that SIMPLE is able to form a ternary complex with STAM1 and Hrs via a direct interaction with STAM1.

Next, we analyzed the colocalization of SIMPLE with STAM1 and Hrs by double immunostaining analysis and found a significant overlap in the distribution of endogenous SIMPLE with STAM1, Hrs, and the early endosome marker Rab5 but not with the ER marker KDEL or the late endosome and lysosome marker LAMP2 (Fig. 1, E–G; and Fig. S1 B), which indicates that a subpopulation of SIMPLE colocalizes with ESCRT-0 components in HeLa cells. Furthermore, triple labeling analysis showed that SIMPLE colocalized with STAM1 and TSG101 on EEA1-positive early endosomes but not on LAMP2-positive late endosomes and lysosomes (Fig. S1, C and D). These results, together with our biochemical data (Fig. 1, B–D), indicate that SIMPLE associates with STAM1, Hrs, and TSG101 on early endosomes.

SIMPLE does not function as an E3 ubiquitin-protein ligase

We were initially intrigued by the hypothesis that SIMPLE might be an E3 ligase because its C-rich domain was thought to be a putative RING finger domain (Moriwaki et al., 2001; Saifi et al., 2005). However, our sequence analysis showed that the C-rich domain of SIMPLE is unlikely to be a RING finger domain because it lacks a key His residue and is interrupted by an embedded transmembrane domain (TMD; Lee et al., 2011). We found that deletion of the TMD from SIMPLE completely disrupted the membrane association of SIMPLE (Fig. S2, A and B), which indicates that the TMD is responsible for anchoring SIMPLE to the membrane. We tested whether SIMPLE has an E3 ligase function by performing in vitro ubiquitination assays and found that SIMPLE had no detectable E3 ligase activity for auto-ubiquitinating (Fig. S2 D) or ubiquitinating STAM1 or TSG101 (Fig. S2, E and F). In contrast, the positive control RING finger protein parkin showed robust E3 ligase activity under the conditions of our in vitro ubiquitination assay (Fig. S2 C). Our coimmunoprecipitation analyses revealed that SIMPLE was unable to interact with the E2 enzymes UbcH5, UbcH7, and UbcH8 in HeLa cells (Fig. S2, G–I). These results provide evidence that SIMPLE does not function as an E3 ligase.

SIMPLE functions in the regulation of endosome-to-lysosome trafficking and signaling attenuation

To identify SIMPLE function, we depleted endogenous SIMPLE in HeLa cells by stable transfection of SIMPLE-targeting shRNAs (Fig. S3, A and B). Immunofluorescence confocal microscopic analyses showed that, in SIMPLE-depleted cells, EEA1-positive early endosomes were significantly larger than those in the control cells (Fig. 2, A–C). In addition, SIMPLE depletion caused clustering of early endosomes in the perinuclear region (Fig. 2, A and D). Because the apparent mean diameter of early endosomes (Fig. 2 B) was near the lateral resolution limit of the confocal microscope, the actual sizes of the early endosomes could not be accurately measured by the confocal microscopy. Therefore, we performed super-resolution imaging analysis of early endosomes by using 3D structured illumination microscopy (3D-SIM; Schermelleh et al., 2008; Huang et al., 2009).

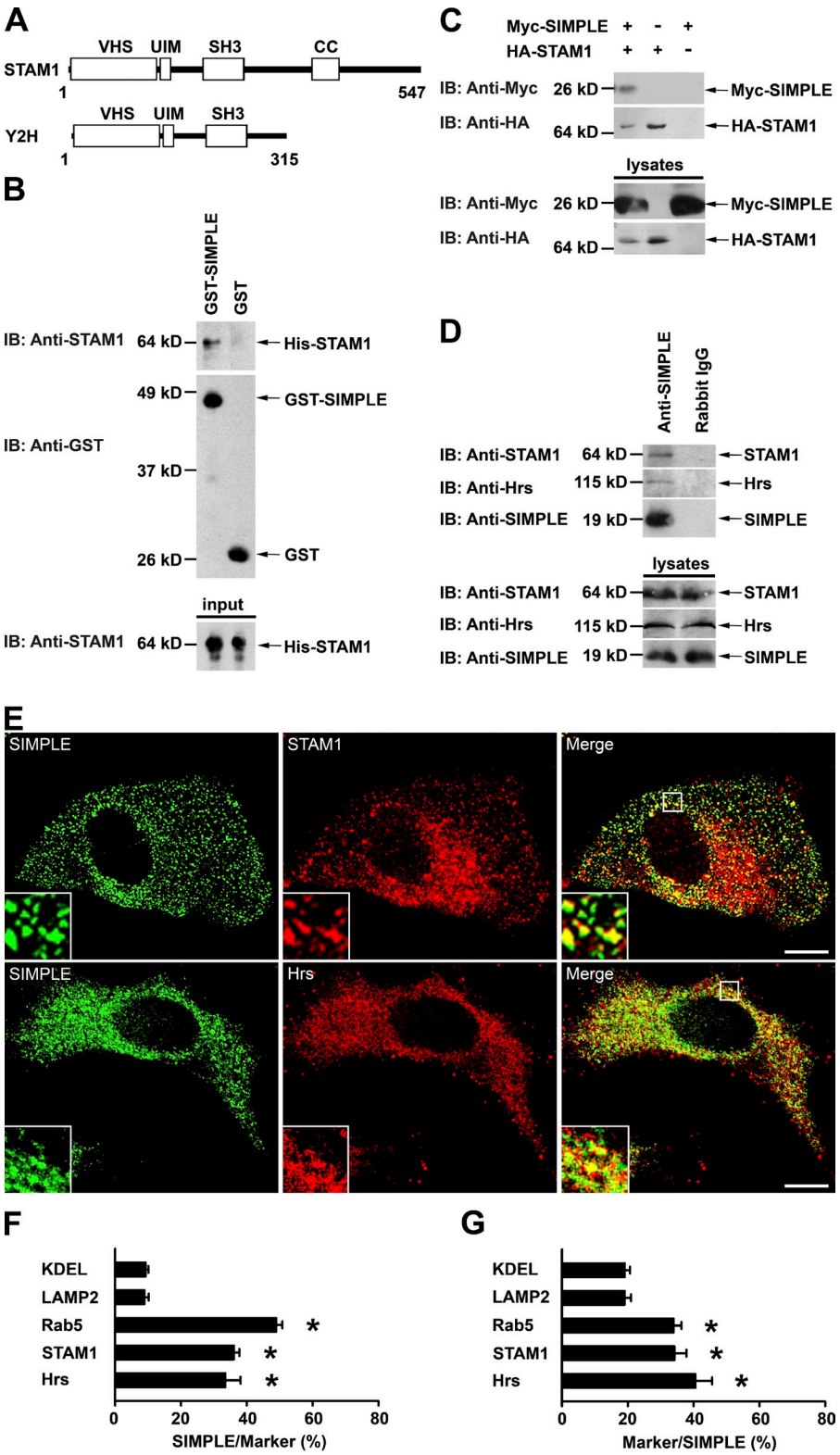

Figure 1. **SIMPLE associates and colocalizes with STAM1 and Hrs.** (A) Domain structure of rat STAM1 (STAM1) and the SIMPLE-interacting clone isolated from yeast two-hybrid screen (Y2H). (B) In vitro binding assays were performed by incubation of soluble His-tagged STAM1 protein (input) with immobilized GST or GST-SIMPLE fusion protein. Bound STAM1 protein was detected by immunoblotting. (C) Lysates from HeLa cells cotransfected with Myc-tagged SIMPLE or empty Myc vector and HA-tagged STAM1 or empty HA vector were immunoprecipitated with anti-HA antibody followed by immunoblot analyses. (D) Association of endogenous SIMPLE with STAM1 and Hrs. HeLa cell lysates were immunoprecipitated with anti-SIMPLE antibody or control rabbit IgG followed by immunoblotting. (E) HeLa cells were double immunostained with antibodies against SIMPLE (green) and STAM1 or Hrs (red). Inset panels show enlarged views of the boxed regions. Bars, 10 µm. (F and G) Quantification of the percentage of SIMPLE overlapping with the indicated markers (F) and the percentage of the indicated marker overlapping with SIMPLE (G) shows a significant colocalization of SIMPLE with STAM1, Hrs, and Rab5. Data represent mean ± SEM (n = 25–38 cells). *, $P < 0.05$ versus the KDEL control, one-way analysis of variance with a Tukey's post hoc test.

Consistent with the enhanced resolving power of 3D-SIM, we found that early endosomes labeled by EEA1 had a considerably smaller size (Fig. 2, E–G) than the one suggested by confocal microscopy (Fig. 2, A–C). In the SIM images of SIMPLE-depleted cells, EEA1-positive early endosomes were often found in small clusters (Fig. 2 E, arrows), and EEA1-positive vacuoles (Fig. 2 E, arrowhead) resembling the enlarged endosomes in Hrs- or STAM-deficient cells (Kanazawa et al., 2003) were occasionally observed. Quantitative analysis indicated a significant increase in the sizes of individual early endosomes in SIMPLE-depleted cells compared with the control cells (Fig. 2, E–G). The endosomal enlargement and clustering induced by SIMPLE depletion are similar to the endosomal morphological phenotypes caused by depletion of STAM, Hrs, or TSG101

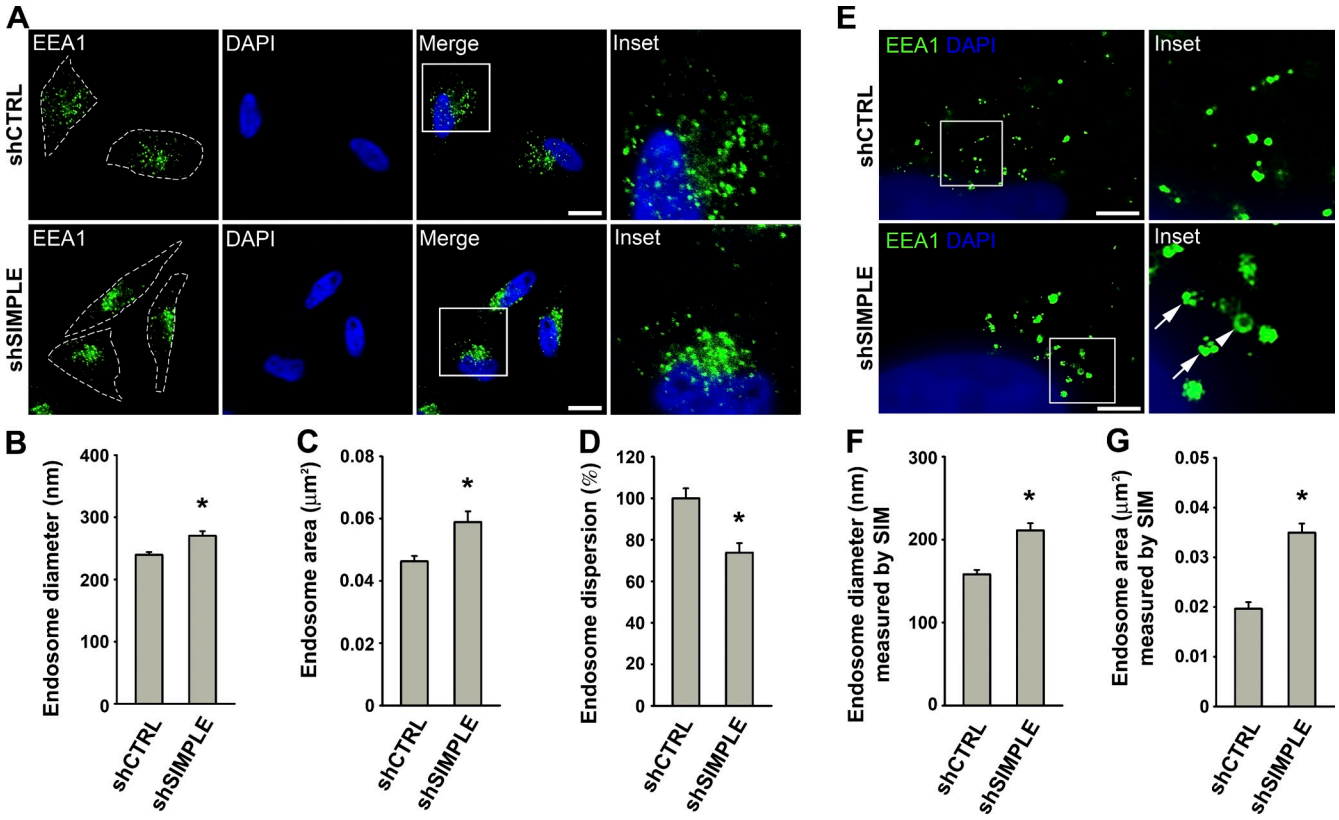

Figure 2. **SIMPLE depletion alters endosomal morphology.** (A–D) Immunofluorescence confocal microscopic analysis (A) with anti-EEA1 antibody (green) and DAPI (blue), and quantification of endosome diameter (B), endosome area (C), and the relative extent of endosome dispersion (D) show altered endosomal morphology and distribution in shSIMPLE-transfected HeLa cells compared with the shCTRL-transfected control. Insets are threefold magnifications of the original image. The broken lines in A indicate the boundary of the cells. Bars, 10 µm. Data represent mean ± SEM (error bars; n = 30–50 cells) from three independent experiments. *, $P < 0.05$ versus the control, unpaired two-tailed Student's t test. (E–G) 3D-SIM analysis (E) of cells stained with anti-EEA1 antibody (green) and DAPI (blue) and quantification of endosome diameter (F) and endosome area (G) show endosomal enlargement in shSIMPLE-transfected HeLa cells compared with the control. Insets are threefold magnifications of the boxed regions in the original images. Arrows indicate small clusters of EEA1-positive endosomes, and the arrowhead indicates an EEA1-positive vacuole. Bar, 2 µm. Data represent mean ± SEM (n = 3). *, $P < 0.05$ versus the control, unpaired two-tailed Student's t test.

(Kanazawa et al., 2003; Doyotte et al., 2005; Razi and Futter, 2006), which suggests that SIMPLE may participate in ESCRT-mediated endosomal trafficking.

Next, we examined the effects of SIMPLE depletion on EGF-induced endocytic trafficking and degradation of endogenous EGF receptor (EGFR; also known as ErbB1) in HeLa cells, a widely used model for studying endocytic trafficking (Sorkin and Goh, 2009). Binding of EGF to EGFR at the cell surface causes endocytosis of the ligand–receptor complex and subsequent sorting at the early endosome for lysosomal degradation (Mellman, 1996a,b; Morino et al., 2004; Kirk et al., 2006). We found that EGF-induced EGFR degradation was significantly decreased in SIMPLE-depleted cells compared with the control cells (Fig. 3, A and B), which indicates that SIMPLE is required for ligand-induced lysosomal degradation of EGFR. Texas red–conjugated EGF (TR-EGF) endocytosis assays revealed that SIMPLE-depleted cells internalized a similar amount of TR-EGF compared with the control cells (Fig. 3, C and E), which indicates that SIMPLE is not involved in EGF-induced endocytosis of ligand-receptor complexes. To determine if SIMPLE depletion affects trafficking of EGF–EGFR complexes after endocytosis, we used a pulse-chase trafficking assay (Li et al., 2002; Kirk et al., 2006) in which cells were allowed to internalize TR-EGF for 15 min and the fate of internalized TR-EGF was monitored after a 1-h chase period. We found that SIMPLE-depleted cells retained significantly more internalized TR-EGF than the control cells after the 1-h chase period (Fig. 3, D and F), and the internalized EGF was partly accumulated in EEA1-positive early endosomes (Fig. 3 F). Together, these results indicate that SIMPLE is required for endosome-to-lysosome trafficking of EGF–EGFR complexes but not their endocytosis.

Given the critical role of endosome-to-lysosome trafficking in the attenuation of EGFR signaling (Waterman and Yarden, 2001), we examined whether SIMPLE depletion could affect the mitogen-activated protein (MAP) kinase signaling downstream of EGF-activated EGFR. Analysis of the kinetics of EGF-dependent activation of MAP kinases (ERK1/2) revealed that SIMPLE depletion had no apparent effect on the onset phase of ERK1/2 phosphorylation but significantly altered the inactivation phase of ERK1/2 phosphorylation, leading to prolonged activation of ERK1/2 signaling (Fig. 3, G and H). Thus, SIMPLE is required for the attenuation of EGFR-activated MAP kinase signaling. The observed defects in EGFR trafficking and signaling caused

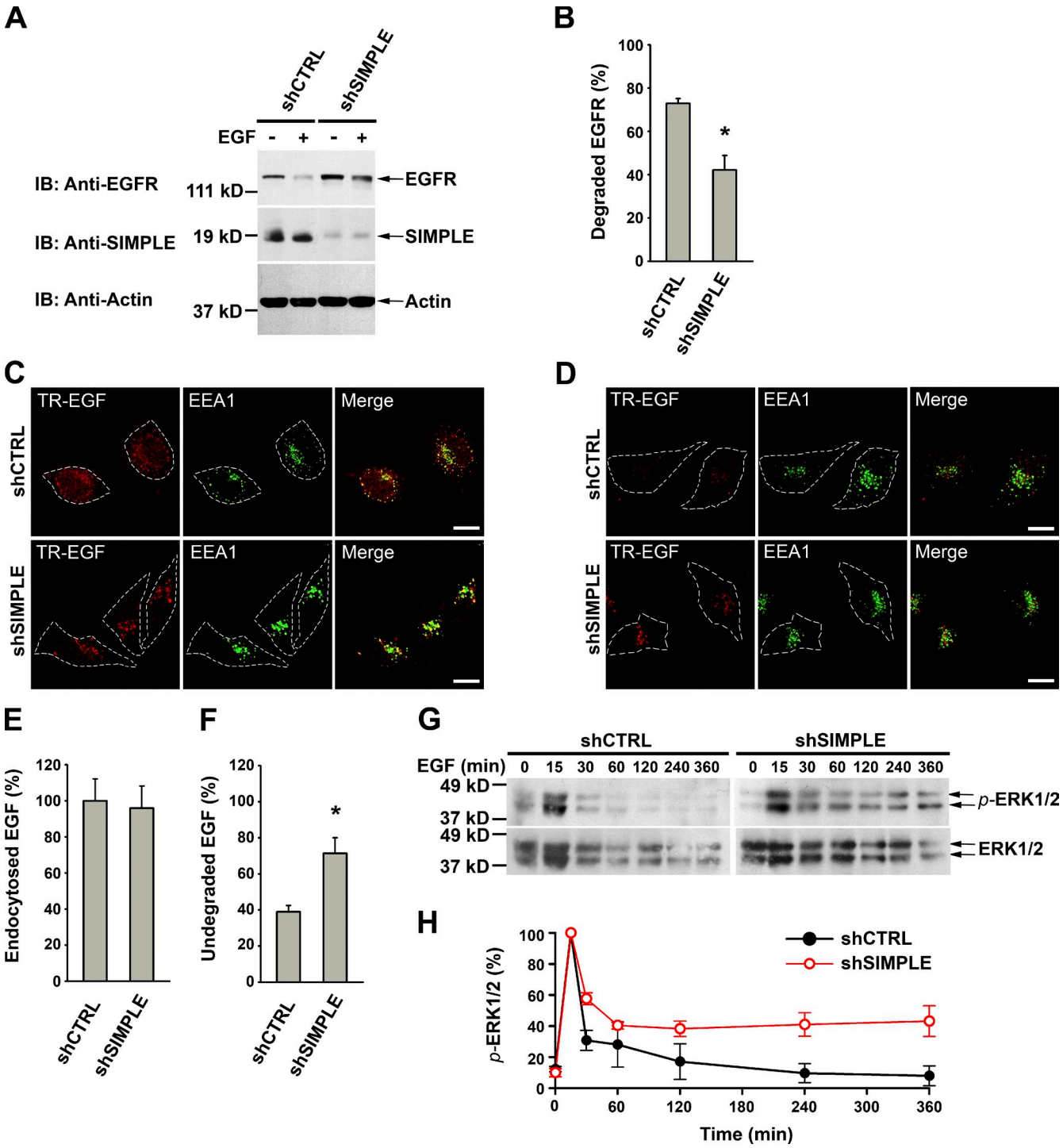

Figure 3. **SIMPLE depletion inhibits EGFR endosomal sorting and signaling.** (A and B) EGFR degradation analysis (A) and quantification (B) show reduced levels of degraded EGFR after treatment with 100 ng/ml EGF for 1 h in shSIMPLE-transfected HeLa cells compared with the shCTRL-transfected control. Data represent mean ± SEM (error bars; $n = 3$). *, $P < 0.05$ versus the control, unpaired two-tailed Student's *t* test. (C and E) TR-EGF endocytosis analysis (C) and quantification (E) show similar amounts of endocytosed TR-EGF (red) after a 15-min incubation with TR-EGF in shSIMPLE-transfected HeLa cells compared with the shCTRL-transfected control. The broken lines in C indicate the boundaries of cells. Bar, 10 µm. Data represent mean ± SEM (error bars; $n = 80–100$ cells) from three independent experiments. (D and F) TR-EGF endosome-to-lysosome trafficking analysis (D) and quantification (F) show accumulation of undegraded TR-EGF (red) on EEA1-positive early endosomes (green) after a 1-h chase of endocytosed TR-EGF in shSIMPLE-transfected HeLa cells compared with the shCTRL-transfected control. Bars, 10 µm. The broken lines in D indicate the boundaries of cells. Data represent mean ± SEM (error bars; $n = 80–120$ cells) from three independent experiments. *, $P < 0.05$ versus the control, unpaired two-tailed Student's *t* test. (G and H) Immunoblot analysis (G) and quantification (H) show levels of phospho-ERK1/2 (*p*-ERK1/2) and total ERK1/2 at the indicated times after treatment with 10 ng/ml EGF in shSIMPLE- or shCTRL-transfected HeLa cells. The *p*-ERK1/2 level was normalized to the ERK1/2 level and plotted as a percentage of the peak value of the normalized *p*-ERK1/2 level. Data represent mean ± SEM (error bars; $n = 3$).

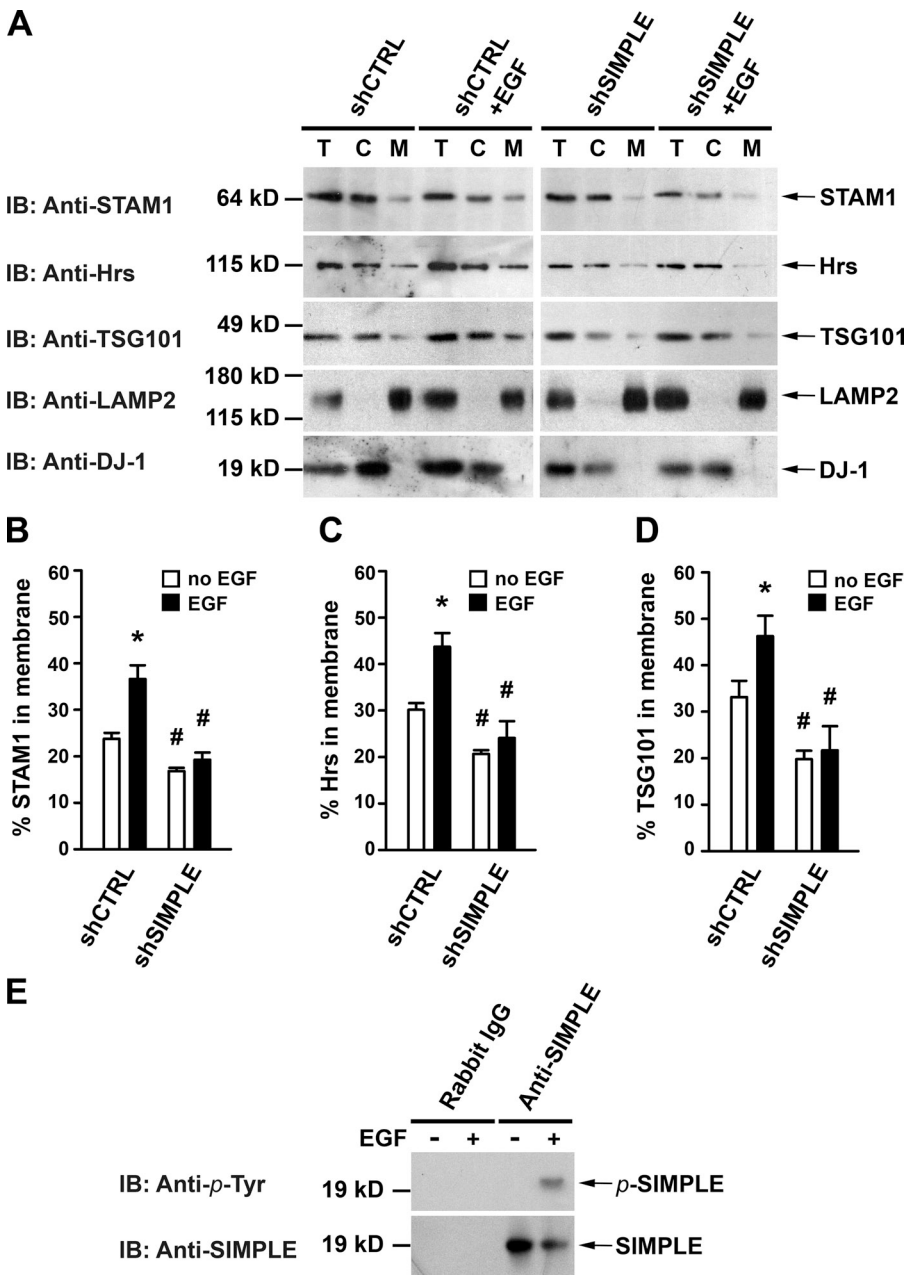

Figure 4. **SIMPLE undergoes EGF-induced tyrosine phosphorylation and is required for efficient association of STAM1, Hrs, and TSG101 with membranes.** (A) Postnuclear supernatant (T) from untreated or EGF (100 ng/ml for 15 min)-treated HeLa cells expressing the indicated shRNAs were separated into cytosol (C) and membrane (M) fractions. Aliquots representing an equal percentage of each fraction were subjected to immunoblot analyses. (B–D) The percentages of STAM1 (B), Hrs (C), and TSG101 (D) in the membrane fraction relative to the total amount in the corresponding postnuclear supernatant (T) were quantified and shown as mean ± SEM from three independent experiments (error bars). *, $P < 0.05$ versus the untreated control; #, $P < 0.05$ versus the corresponding shCTRL, two-way analysis of variance with a Tukey's post hoc test. (E) Tyrosine phosphorylation of endogenous SIMPLE in untreated or EGF (100 ng/ml for 15 min)-treated HeLa cells was determined by immunoprecipitation with anti-SIMPLE antibody followed by immunoblotting using anti–phospho-tyrosine and anti-SIMPLE antibodies. Immunoprecipitation with rabbit IgG was used as a negative control.

by SIMPLE depletion are similar to the phenotypes seen upon depletion of ESCRT-0 or ESCRT-I subunits (Babst et al., 2000; Bache et al., 2004; Doyotte et al., 2005), and provide functional evidence supporting a role of SIMPLE in the regulation of endosomal sorting and trafficking.

SIMPLE promotes recruitment of STAM1, Hrs, and TSG101 to membranes

Our finding that SIMPLE is an early endosomal membrane protein (Lee et al., 2011) that interacts and colocalizes with STAM1, Hrs, and TSG101 (Fig. 1 and Fig. S1, C and D) raises the possibility that SIMPLE may participate in the recruitment of these ESCRT subunits to endosomal membranes. To examine this possibility, we performed subcellular fractionation analysis to assess the effects of SIMPLE depletion on membrane association of endogenous STAM1, Hrs, and TSG101 in HeLa cells. We found that, in the control cells, a small pool of these ESCRT components were associated with membranes under the normal cell culture condition (Fig. 4, A–D), which is in agreement with previous studies (Bache et al., 2003a,b). In response to EGF stimulation, more STAM1, Hrs, and TSG101 proteins were recruited to membranes in the control cells (Fig. 4, A–D). SIMPLE depletion resulted in significant decreases in the levels of membrane-associated STAM1, Hrs, and TSG101 under both the normal and EGF-stimulated conditions (Fig. 4, A–D), which indicates that SIMPLE is essential for efficient recruitment of these ESCRT components to membranes. We found that SIMPLE depletion did not cause any significant change in the steady-state level of STAM1, Hrs, or TSG101 (Fig. S3, C–F), which indicates a lack of effect of SIMPLE depletion on the stability of these ESCRT proteins. Collectively, these results suggest that the impaired endosome-to-lysosome

trafficking in SIMPLE-depleted cells (Fig. 3) is caused by reduced membrane recruitment of STAM1, Hrs, and TSG101 rather than reduced levels of these ESCRT proteins.

SIMPLE undergoes tyrosine phosphorylation in response to EGF stimulation

The observed SIMPLE-dependent, enhanced membrane recruitment of STAM1, Hrs, and TSG101 under the EGF-stimulated conditions (Fig. 4, A–D) prompted us to test whether SIMPLE is tyrosine-phosphorylated in response to EGF stimulation. In vivo phosphorylation analysis revealed that, although no tyrosine phosphorylation of endogenous SIMPLE in HeLa cells was detectable under the normal cell culture condition, robust tyrosine phosphorylation of SIMPLE was induced by EGF stimulation (Fig. 4 E). The EGF-induced phosphorylation of SIMPLE might provide a mechanism for enhancing the ability of SIMPLE to promote membrane recruitment of STAM1, Hrs, and TSG101 under the EGF-stimulated conditions.

SIMPLE interaction with TSG101 is required for endosome-to-lysosome trafficking

SIMPLE contains a PSAP tetrapeptide motif for binding TSG101 (Fig. 5 A), and mutation of this motif abolished the interaction of SIMPLE with TSG101 (Shirk et al., 2005). To determine the functional role of SIMPLE interaction with TSG101, we changed the PSAP motif of SIMPLE to ASAA by site-directed mutagenesis. We took advantage of the SIMPLE depletion phenotype (Fig. 3) and performed rescue experiments with shRNA-resistant SIMPLE wild type (WT) and SIMPLE ASAA mutants, and assessed their abilities to rescue EGFR trafficking defects in SIMPLE-depleted cells. Western blot analysis confirmed that the expression levels of exogenous SIMPLE proteins were comparable to the level of endogenous SIMPLE protein (Fig. S3 G). We found that the defective EGFR trafficking phenotype of SIMPLE depletion was rescued by SIMPLE WT (Fig. 5, B-E), confirming that the observed trafficking defects in SIMPLE-depleted cells were caused specifically by the loss of SIMPLE but not off-target effects of shRNAs. SIMPLE ASAA mutant was much less effective than SIMPLE WT in rescuing EGFR trafficking defects in SIMPLE-depleted cells (Fig. 5, B–E), which indicates that mutation of the SIMPLE PSAP motif causes impairment in SIMPLE function. These results support an essential role for the interaction of SIMPLE with TSG101 in the control of endosome-to-lysosome trafficking.

SIMPLE and Hrs have nonredundant roles in regulating endosome-to-lysosome trafficking

Because SIMPLE and Hrs share the ability to bind STAM1 and TSG101 and regulate endosome-to-lysosome trafficking, we performed rescue experiments to examine whether overexpression of Hrs could ameliorate the defective EGFR degradative trafficking phenotype of SIMPLE depletion. We found that overexpression of Hrs was unable to rescue the EGF-induced EGFR degradation defect in SIMPLE-depleted cells (Fig. S4, A and B). As we and others have previously reported (Chin et al., 2001; Raiborg et al., 2001; Urbé et al., 2003), overexpression of Hrs caused an inhibition of EGF-induced EGFR degradation in control cells (Fig. S4, A and B). We also performed reciprocal analyses to assess the effect of overexpression of SIMPLE in Hrs-depleted cells and found that overexpression of SIMPLE was unable to rescue the EGFR degradation defect caused by Hrs depletion (Fig. S4, C and D). Unlike Hrs, overexpression of SIMPLE had no effect on EGF-induced EGFR degradation in control cells (see Fig. 7, A and B). Together, these results support the finding that SIMPLE and Hrs have nonredundant roles in regulating endosome-to-lysosome trafficking.

CMT1C-linked SIMPLE mutants impair endosomal trafficking via a loss-of-function, dominant-negative mechanism

Human genetic studies have identified eight CMT1C-linked SIMPLE mutations, which mapped within or around the TMD of SIMPLE (Fig. 5 A). To determine the effects of CMT1C-linked mutations on SIMPLE function, we focused on two representative SIMPLE mutations: W116G, which locates in the middle of a cluster of five mutations near the N terminus of the TMD; and P135T, which is one of the two mutations at the C terminus of the TMD (Fig. 5 A). We performed rescue experiments by expressing shRNA-resistant SIMPLE mutants along with SIMPLE WT in SIMPLE-depleted cells at similar levels to that of endogenous SIMPLE (Fig. S3 G) and assessed their abilities to rescue the SIMPLE depletion phenotype. Our results revealed that, although SIMPLE WT was able to rescue the defective EGFR trafficking phenotype of SIMPLE depletion, this ability was abrogated by SIMPLE W116G and P135T mutations (Fig. 6). These results support the finding that the CMT1C-linked SIMPLE mutants are loss-of-function mutants that are unable to facilitate endosome-to-lysosome trafficking.

Because SIMPLE mutations cause autosomal dominant CMT1C, we investigated whether SIMPLE W116G and P135T mutations have dominant-negative effects on endosome-to-lysosome trafficking. We found that expression of exogenous SIMPLE W116G or P135T mutant, but not SIMPLE WT (Fig. S5 A), significantly impaired EGF-induced EGFR degradation (Fig. 7, A and B) and TR-EGF trafficking in cells (Fig. 7, C and D), which indicates a dominant-negative role for the CMT1C-linked SIMPLE mutants in endosome-to-lysosome trafficking.

We then performed biochemical analyses to explore the potential mechanism underlying the observed dominant-negative effects of SIMPLE mutants. Coimmunoprecipitation analysis (Fig. 8 A) and GST pull-down assays (Fig. 8 C) revealed that SIMPLE WT has the ability to self-associate, which suggests that SIMPLE may function as a homodimer in cells. We found that SIMPLE self-association was abolished by deletion of its C-rich domain but not by deletion of its N-terminal proline-rich region (Fig. 8, B and C), which indicates that the C-rich domain is required for SIMPLE self-association. Our pull-down assays showed that SIMPLE W116G and P135T mutants were capable of binding SIMPLE WT (Fig. 8 D). CMT1C-linked SIMPLE mutants have been reported to retain the ability to interact with

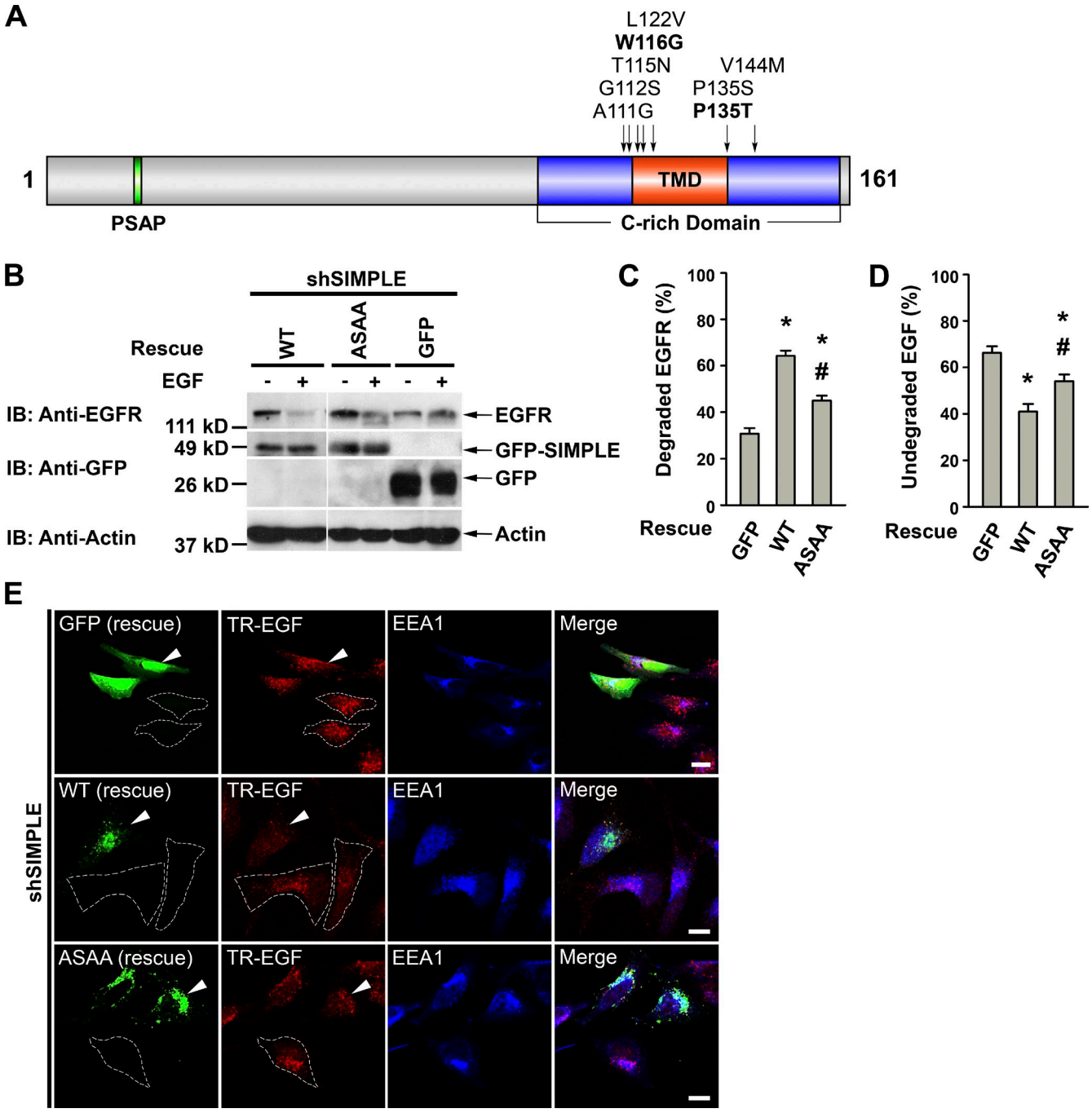

Figure 5. **SIMPLE interaction with TSG101 is required for ligand-induced EGFR degradation and EGF endosome-to-lysosome trafficking.** (A) Domain structure of SIMPLE. The locations of the PSAP motif and CMT1C-linked SIMPLE mutations are indicated on the domain structure. (B–E) SIMPLE-depleted HeLa cells with shSIMPLE were "rescued" by transfection with shSIMPLE-resistant SIMPLE WT and SIMPLE ASAA mutant or GFP control. Analysis of EGF (100 ng/ml for 1 h)-induced EGFR degradation (B) and quantification (C) show that SIMPLE ASAA mutant is much less effective than SIMPLE WT in rescuing the EGFR degradation phenotype of SIMPLE-depleted cells. Data represent mean ± SEM (error bars; $n = 3$). *, $P < 0.05$ versus the GFP control; #, $P < 0.05$ versus SIMPLE WT, one-way analysis of variance with a Tukey's post hoc test. TR-EGF endosome-to-lysosome trafficking analysis (E) and quantification (D) show more accumulation of undegraded TR-EGF (red) on EEA1-positive early endosomes (blue) after a 1-h chase of endocytosed TR-EGF in SIMPLE ASAA-rescued cells (green) than that in the SIMPLE WT-rescued cells (green). Data represent mean ± SEM (error bars; $n = 50–80$ cells) from three independent experiments. *, $P < 0.05$ versus the GFP control; #, $P < 0.05$ versus SIMPLE WT, one-way analysis of variance with a Tukey's post hoc test. The broken lines in E indicate the boundaries of nonrescued cells, and the arrowheads indicate rescued cells. Bars, 10 µm.

TSG101 (Shirk et al., 2005), and we found that the SIMPLE mutants also retained the ability to interact with STAM1 (Fig. 8 E). We have previously shown that SIMPLE W116G and P135T mutations cause mislocalization of SIMPLE from the endosomal membrane to the cytosol (Lee et al., 2011), and our coimmunoprecipitation analyses with cytosolic fractions of HeLa cells revealed that the cytosolic SIMPLE mutants retain the ability to bind STAM1, Hrs, and TSG101 (Fig. 8 F). In addition, we found that expression of exogenous SIMPLE W116G or P135T mutant, but not SIMPLE WT (Fig. S5 A), significantly

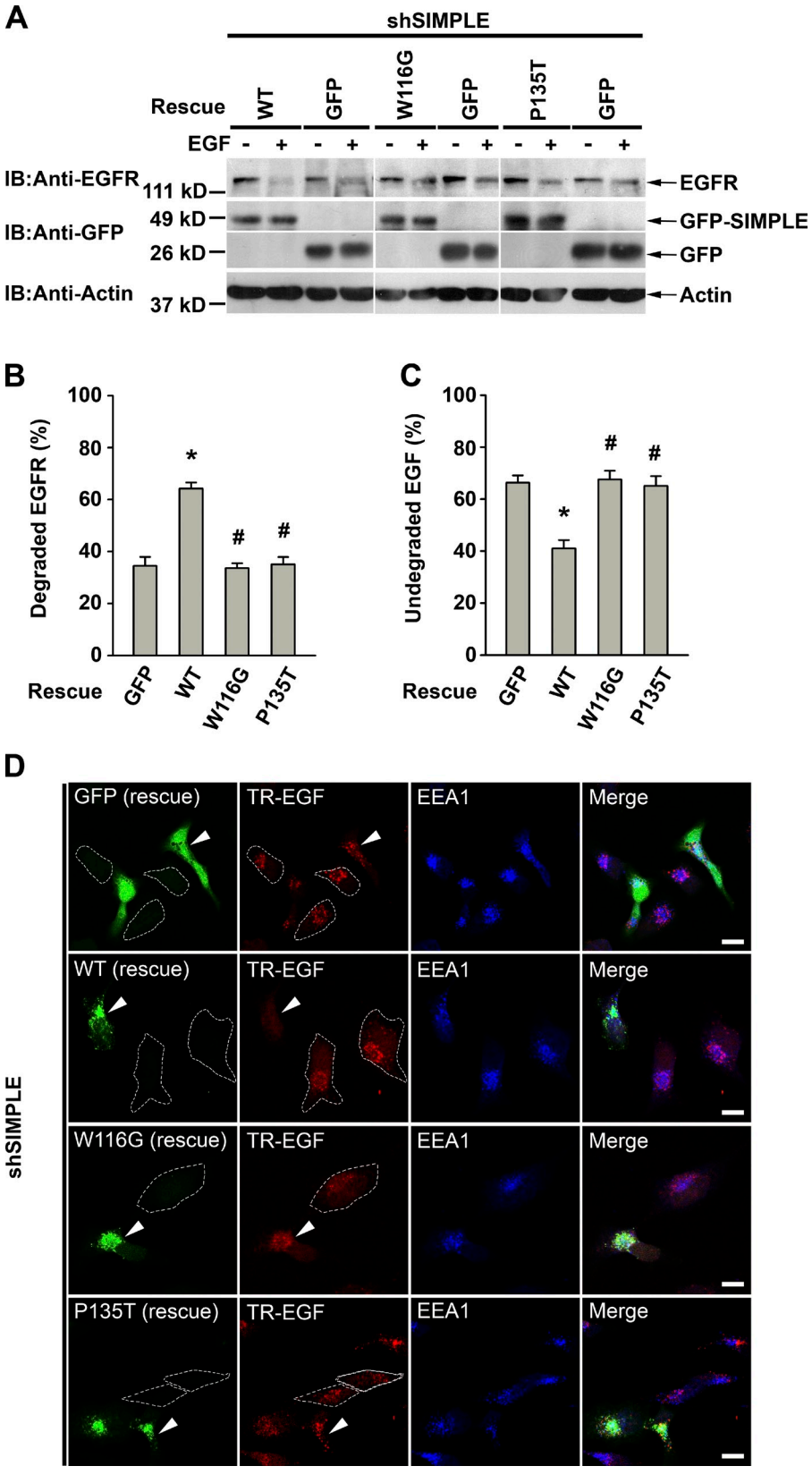

Figure 6. **CMT1C-linked mutations cause a loss of SIMPLE function in facilitating EGFR degradation and EGF endosome-to-lysosome trafficking.** SIMPLE-depleted HeLa cells with shSIMPLE were "rescued" by transfection with shSIMPLE-resistant SIMPLE WT, SIMPLE W116G, SIMPLE P135T, or GFP control. (A and B) Analysis of EGF (100 ng/ml for 1 h)-induced EGFR degradation (A) and quantification (B) shows that SIMPLE W116G and SIMPLE P135T are much less effective than SIMPLE WT in rescuing the EGFR degradation phenotype of SIMPLE-depleted cells. Data represent mean ± SEM from at least three independent experiments (error bars). *, $P < 0.05$ versus the GFP control; #, $P < 0.05$ versus SIMPLE WT, one-way analysis of variance with a Tukey's post hoc test. (C and D) TR-EGF endosome-to-lysosome trafficking analysis (D) and quantification (C) show more accumulation of undegraded TR-EGF (red) on EEA1-positive early endosomes (blue) after a 1-h chase of endocytosed TR-EGF in SIMPLE W116G- or SIMPLE P135T-rescued cells (green) than that in the SIMPLE WT-rescued cells (green). Data represent mean ± SEM (error bars; $n = 50–80$ cells) from three independent experiments. *, $P < 0.05$ versus the GFP control; #, $P < 0.05$ versus SIMPLE WT, one-way analysis of variance with a Tukey's post hoc test. The broken lines in D indicate the boundaries of nonrescued cells, and the arrowheads indicate rescued cells. Bars, 10 µm.

impaired the recruitment of STAM1, Hrs, and TSG101 to membranes (Fig. 9). These findings, together with the results of functional analyses (Figs. 6 and 7), suggest that the mislocalized SIMPLE mutants in the cytosol compete with endosome-localized, endogenous SIMPLE for binding STAM1, Hrs, and TSG101, thus acting in a dominant-negative manner to inhibit the recruitment to these ESCRT proteins to endosomal membranes, leading to impaired endosome-to-lysosome trafficking.

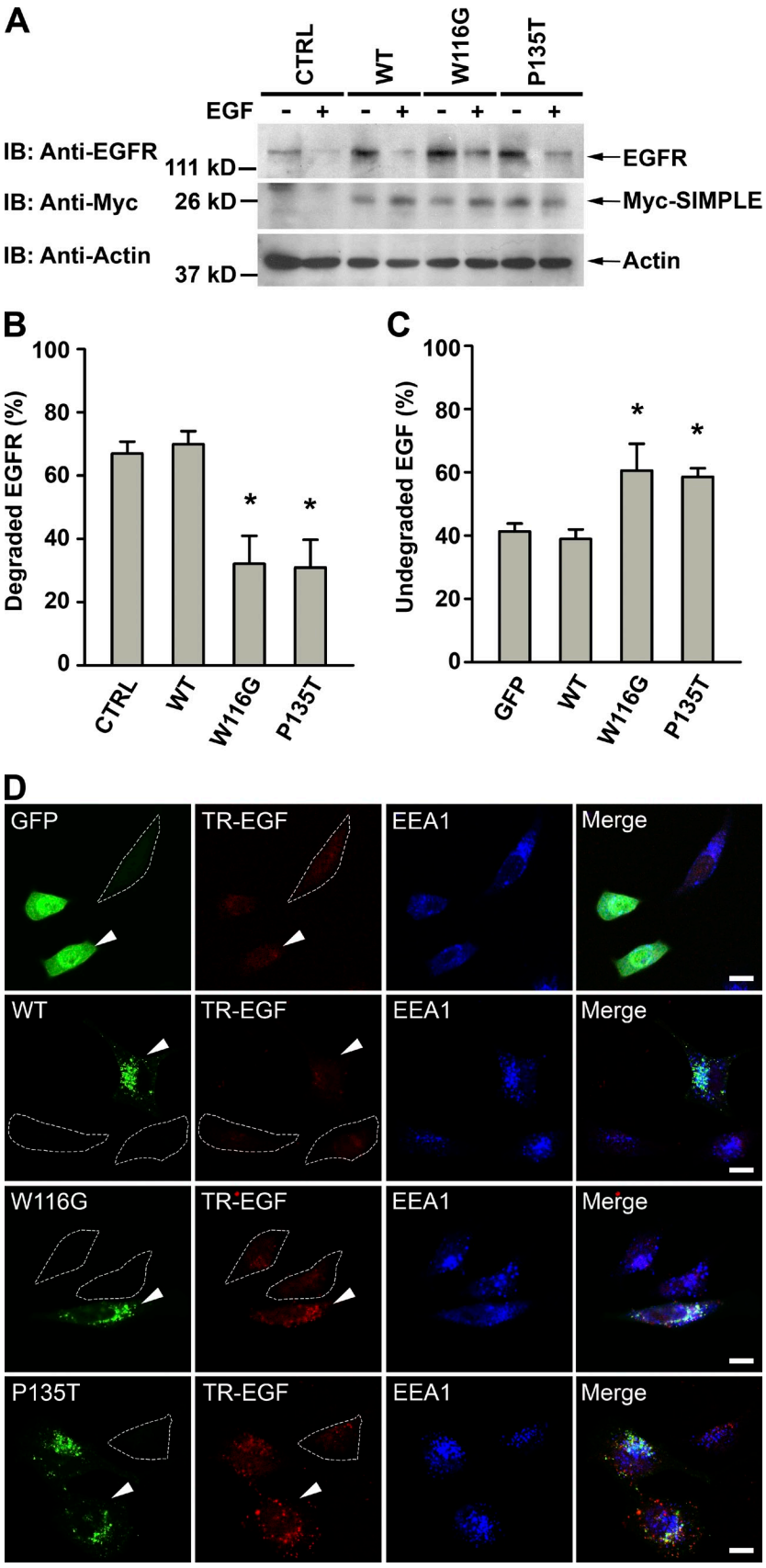

Figure 7. **CMT1C-linked SIMPLE mutants have dominant-negative effects on EGFR degradation and EGF endosome-to-lysosome trafficking.** (A and B) HeLa cells expressing the indicated Myc-tagged SIMPLE WT or mutant, or Myc vector control (CTRL) were incubated with or without 100 ng/ml EGF for 1 h. EGFR degradation analysis (A) and quantification (B) show reduced levels of degraded EGFR in SIMPLE W116G– or SIMPLE P135T–transfected cells compared with SIMPLE WT-transfected cells or the Myc vector control. Data represent mean ± SEM from at least three independent experiments (error bars). *, $P < 0.05$ versus SIMPLE WT or the vector control, one-way analysis of variance with a Tukey's post hoc test. (C and D) TR-EGF endosome-to-lysosome trafficking analysis (D) and quantification (C) show more accumulation of undegraded TR-EGF (red) on EEA1-positive early endosomes (blue) after 1-h chase of endocytosed TR-EGF in GFP-tagged SIMPLE W116G– or SIMPLE P135T–transfected cells (green) than that in the GFP-tagged SIMPLE WT- or GFP-transfected cells (green). Data represent mean ± SEM (error bars; $n = 50–80$ cells) from three independent experiments. *, $P < 0.05$ versus SIMPLE WT or the vector control, one-way analysis of variance with a Tukey's post hoc test. The broken lines in D indicate the boundaries of nontransfected cells, and the arrowheads indicate transfected cells. Bars, 10 µm.

CMT1C-linked SIMPLE mutants cause dysregulation of neuregulin-1 (NRG1)-ErbB signaling in Schwann cells

NRG1 signaling through ErbB receptor tyrosine kinases has emerged as a major pathway for controlling myelination of peripheral nerves by Schwann cells (Chen et al., 2006; Syed et al., 2010). Our finding of abundant expression of SIMPLE in Schwann cells (Lee et al., 2011) prompted us to determine whether SIMPLE has a role in the regulation of NRG1-ErbB signaling in Schwann cells. Only two members of the ErbB family of receptors, ErbB2 and ErbB3, are expressed in Schwann cells (Nave and Salzer, 2006; Newbern and Birchmeier, 2010). In response to NRG1 binding, ErbB2 and ErbB3 form heterodimers, leading to receptor cross-phosphorylation and activation of downstream signaling pathways (Nave and Salzer, 2006; Birchmeier, 2009; Quintes et al., 2010). Like EGFR/ErbB1, ligand-induced activation causes ErbB3 endocytosis and subsequent degradation by the lysosome, although the ErbB3 degradation occurs at a slower rate than that of EGFR (Cao et al., 2007; Sorkin and Goh, 2009). To investigate the function of SIMPLE in Schwann cells, we depleted endogenous SIMPLE in MSC80 mouse Schwann cells by stable transfection of SIMPLE-targeting shRNAs (Fig. S5 B). We found that NRG1-induced ErbB3 down-regulation was significantly decreased in SIMPLE-depleted Schwann cells compared with the control cells (Fig. 10, A and B), which indicates that SIMPLE is required for NRG1-induced lysosomal degradation of ErbB3. Analysis of ERK1/2 signaling downstream of NRG1-activated ErbB2/ErbB3 receptors revealed that SIMPLE depletion altered the inactivation phase of ERK1/2 phosphorylation, leading to prolonged activation of ERK1/2 signaling (Fig. 10, C and D). These results support a role for SIMPLE in controlling the duration of NRG1-ErbB signaling in Schwann cells.

To determine the effects of CMT1C-linked mutations on NRG1-ErbB signaling in Schwann cells, we expressed Myc-tagged SIMPLE WT, SIMPLE W116G, or SIMPLE P135T in MSC80 Schwann cells by stable transfection (Fig. S5 C) and analyzed their effects on ERK1/2 signaling downstream of NRG1-activated ErbB2/ErbB3 receptors. We found that expression of exogenous SIMPLE W116G or P135T mutant, but not SIMPLE WT, caused prolonged activation of ERK1/2 signaling (Fig. 10, E and F). The altered NRG1-dependent ERK1/2 activation induced by SIMPLE W116G and P135T mutations (Fig. 10, E and F) is similar to the phenotype seen upon depletion of SIMPLE (Fig. 10, C and D), providing additional evidence supporting the dominant-negative pathogenic mechanism of CMT1C-linked SIMPLE mutations.

Discussion

Despite the identification of SIMPLE mutations as the cause of CMT1C (Street et al., 2003; Campbell et al., 2004; Saifi et al., 2005; Latour et al., 2006; Gerding et al., 2009), very little is known about the biochemical function and cellular role of SIMPLE. The present study provides evidence that SIMPLE does not function as an E3 ligase as previously hypothesized (Moriwaki et al., 2001; Saifi et al., 2005). Our findings reveal that SIMPLE is a novel regulator of endosome-to-lysosome trafficking.

Current models of endosomal sorting propose that Hrs, which is localized to the early endosome via an interaction with phosphatidylinositol-3-phosphate (PI(3)P), recruits STAM1 from the cytosol to form the ESCRT-0 complex on the endosomal membrane. The ESCRT-0 initiates the sorting process by concentrating ubiquitinated cargo in the clathrin-coated microdomain of the endosome. Hrs uses its PSAP motif to bind TSG101, leading to recruitment of ESCRT-I, -II, and -III complexes to facilitate cargo transport into multivesicular bodies for lysosomal degradation (Roxrud et al., 2010; Henne et al., 2011). However, previous studies have shown that STAM1 can localize to the endosomal membrane in fibroblast cells derived from Hrs knockout mouse embryos (Kanazawa et al., 2003) and that depletion of Hrs only inhibits membrane association of TSG101 by 50% (Bache et al., 2003a), which suggests that additional mechanisms exist to mediate membrane association of STAM1 and TSG101. Interestingly, our analyses show that the early endosomal membrane protein SIMPLE binds directly to both STAM1 and TSG101 and that SIMPLE is required for efficient membrane association of these proteins. Furthermore, mutation of the TSG101-binding PSAP motif of SIMPLE causes an inhibition of ligand-induced EGFR endosome-to-lysosome trafficking. Together, these results indicate that the direct interaction of SIMPLE with STAM1 and TSG101 provides a mechanism for mediating membrane recruitment of these ESCRT proteins to facilitate endosomal sorting.

Although SIMPLE and Hrs both interact physically with STAM1 and TSG101 and are required for their membrane recruitment, our rescue experiments reveal that SIMPLE and Hrs have nonredundant roles in regulating endosome-to-lysosome trafficking. Unlike Hrs, SIMPLE does not contain any motif or domain for binding clathrin and ubiquitin, and is thus unlikely to directly mediate cargo sorting. Furthermore, unlike Hrs, which forms a 1:1 heterodimeric complex with STAM1 both in the cytosol and on membranes (Bache et al., 2003b) and has an essential role in maintaining the stability of STAM1 (Kanazawa et al., 2003; Mizuno et al., 2004), SIMPLE is an early endosomal membrane protein and has no influence on the stability of STAM1. Previous studies have shown that, although the interaction of Hrs with PI(3)P is involved in recruiting Hrs to the early endosomal membrane, Hrs is predominantly localized to endosomal regions that contain little PI(3)P (Gillooly et al., 2003), which suggests that additional mechanisms exist to mediate membrane association of Hrs. Interestingly, our analyses reveal that, although SIMPLE does not directly interact with Hrs, SIMPLE is able to form a ternary complex with STAM1 and Hrs via direct binding to STAM1, and that SIMPLE is required for efficient membrane association of Hrs, supporting a role for SIMPLE in mediating membrane recruitment of Hrs. Our finding of the ability of SIMPLE to self-associate and to recruit STAM1, Hrs, and TSG101 to the endosomal membrane suggests that SIMPLE may promote the assembly of higher order (multimeric) structures of ESCRT-0 and/or assembly of a "supercomplex" of ESCRT machinery on the membrane to facilitate cargo sorting.

Endosome-to-lysosome trafficking of cell surface receptors is a major mechanism for controlling the intensity and duration

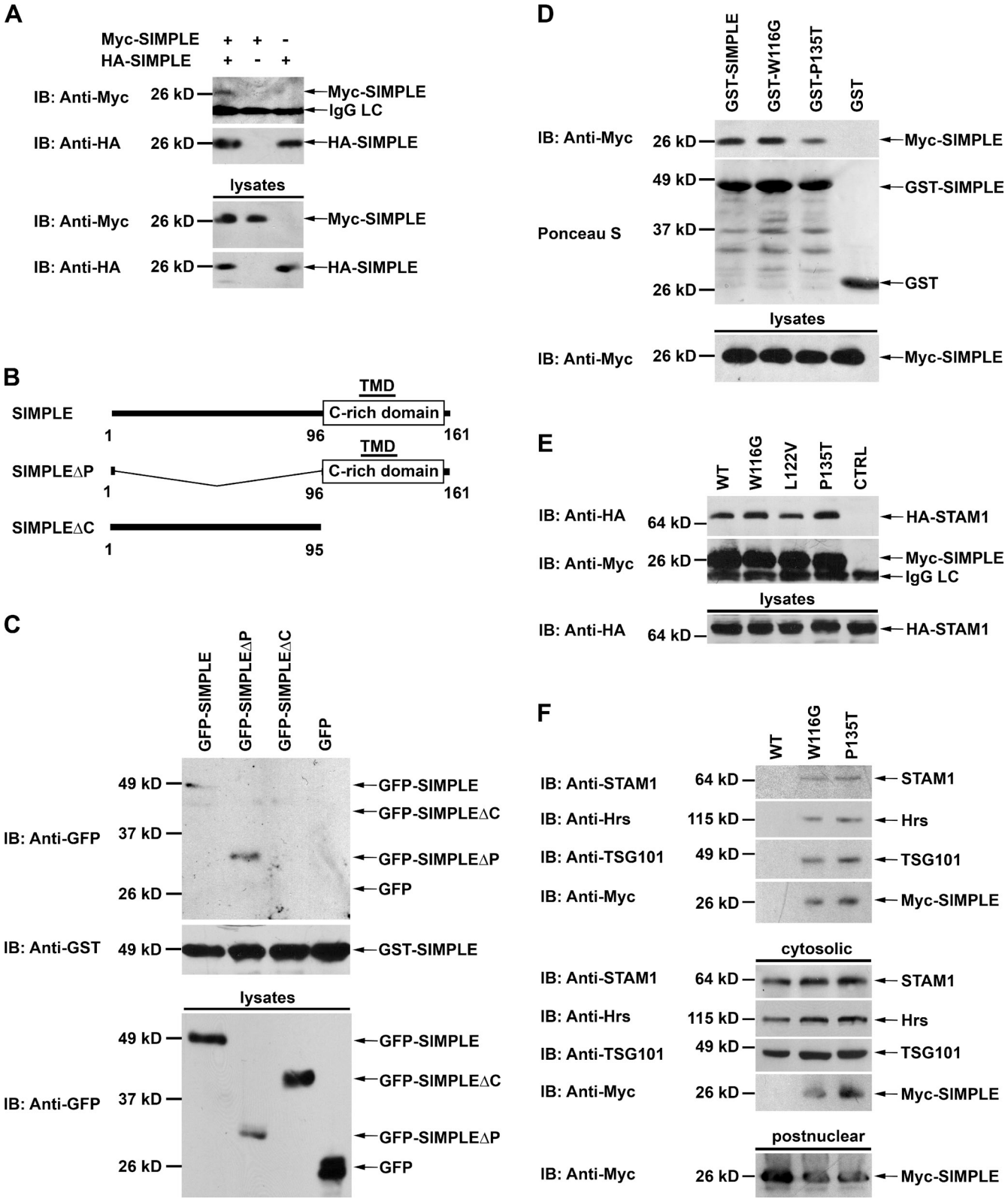

Figure 8. **CMT1C-linked SIMPLE mutants interact with SIMPLE WT, STAM1, Hrs, and TSG101.** (A) SIMPLE self-association in cells. Lysates from HeLa cells expressing Myc-tagged SIMPLE or empty Myc vector and HA-tagged SIMPLE or empty HA vector were immunoprecipitated with anti-HA antibody followed by immunoblot analyses. (B) Schematic illustrating SIMPLE and its deletion mutants encoded by GFP-tagged cDNA constructs. (C) The C-rich domain is required for SIMPLE self-association. GST pull-down assays were performed by incubation of immobilized GST-tagged SIMPLE with lysates of HeLa cells expressing the indicated GFP-tagged SIMPLE proteins or GFP control. Bound proteins were detected by immunoblotting. (D) Interaction of SIMPLE mutants with SIMPLE WT. GST pull-down assays were performed by incubation of immobilized GST-tagged SIMPLE WT, SIMPLE W116G, SIMPLE P135T, or GST control with lysates of HeLa cells expressing Myc-tagged SIMPLE WT. Bound SIMPLE protein was detected by immunoblotting. (E) Interaction of SIMPLE mutants with STAM1. Lysates from HeLa cells cotransfected with HA-tagged STAM1 and the indicated Myc-tagged SIMPLE WT, mutant, or Myc vector

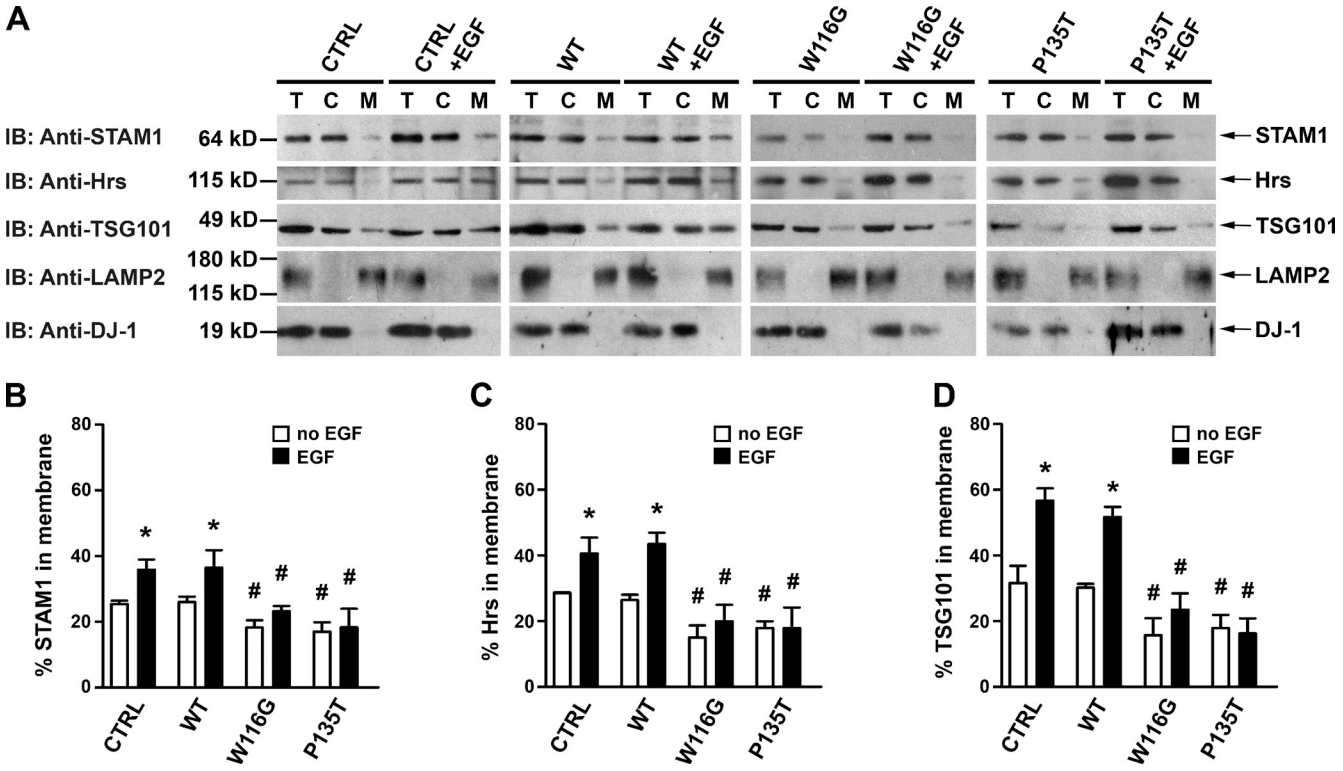

Figure 9. **CMT1C-linked SIMPLE mutants inhibit membrane association of STAM1, Hrs, and TSG101.** (A) Postnuclear supernatant (T) from untreated or EGF (100 ng/ml for 15 min)-treated HeLa cells expressing Myc-tagged SIMPLE WT, SIMPLE W116G, SIMPLE P135T, or Myc vector control (CTRL) were separated into cytosol (C) and membrane (M) fractions. Aliquots representing an equal percentage of each fraction were subjected to immunoblot analyses. (B–D) The percentages of STAM1 (B), Hrs (C), and TSG101 (D) in the membrane fraction relative to the total amount in the corresponding postnuclear supernatant were quantified and shown as mean ± SEM from three independent experiments (error bars). *, $P < 0.05$ versus the corresponding untreated control; #, $P < 0.05$ versus the corresponding vector control or WT-expressing cells, two-way analysis of variance with a Tukey's post hoc test.

of signal transduction in cells (Waterman and Yarden, 2001; Katzmann et al., 2002). ESCRT-mediated endosomal sorting of signaling receptors has been shown to play a crucial role in attenuation of signal transduction (Wegner et al., 2011). Consistent with the essential role of SIMPLE in regulation of endosomal sorting and trafficking, our study reveals that SIMPLE is required for efficient attenuation of ERK1/2 signaling downstream of EGF-activated EGFR. In addition, SIMPLE is also required for efficient attenuation of ERK1/2 signaling downstream of NRG1-activated ErbB2/ErbB3 receptors. Our findings indicate that SIMPLE acts as a regulator of cell signaling by mediating ligand-induced receptor degradation.

The importance of SIMPLE is underscored by the linkage of SIMPLE mutations to autosomal dominant CMT1C (Street et al., 2003; Campbell et al., 2004; Saifi et al., 2005; Latour et al., 2006; Gerding et al., 2009). We have recently shown that SIMPLE is a posttranslationally inserted, early endosomal membrane protein and that CMT1C-linked SIMPLE mutations impair the membrane insertion of SIMPLE, causing it to mislocalize from the endosomal membrane to the cytosol (Lee et al., 2011). The present study is the first to examine the functional consequences of CMT1C-linked SIMPLE mutations. Our finding of the inability of SIMPLE W116G and P135T mutants to rescue the SIMPLE depletion phenotype indicates that the CMT1C-linked SIMPLE mutants are loss-of-function mutants that are incapable of facilitating endosome-to-lysosome trafficking. This finding is consistent with the notion that mutation-induced mislocalization removes SIMPLE from its site of action, causing a loss of SIMPLE function in regulating endosomal trafficking. Furthermore, our analyses reveal that SIMPLE W116G and P135T mutants retain the ability to bind STAM1, Hrs, and TSG101 and exert a dominant-negative effect on their membrane recruitment and endosome-to-lysosome trafficking. These results support the model that the mislocalized SIMPLE mutants in the cytosol compete with endogenous SIMPLE for binding STAM1, Hrs, and TSG101, thus acting in a dominant-negative manner to inhibit membrane recruitment of these ESCRT proteins and thereby impair endosomal sorting and trafficking. Collectively, these findings support a loss-of-function, dominant-negative pathogenic mechanism by which heterozygous SIMPLE mutations cause autosomal dominant CMT1C.

Our study reveals a link between dysregulated endosome-to-lysosome trafficking and the pathogenesis of demyelinating

(CTRL) were subjected to immunoprecipitation with anti-Myc antibody followed by immunoblot analyses. (F) Interaction of SIMPLE mutants with STAM1, Hrs, and TSG101 in the cytosol. Cytosolic fractions of transfected HeLa cells expressing the indicated Myc-tagged SIMPLE WT or mutant were subjected to immunoprecipitation with anti-Myc antibody followed by immunoblot analysis. IgG LC, IgG light chain.

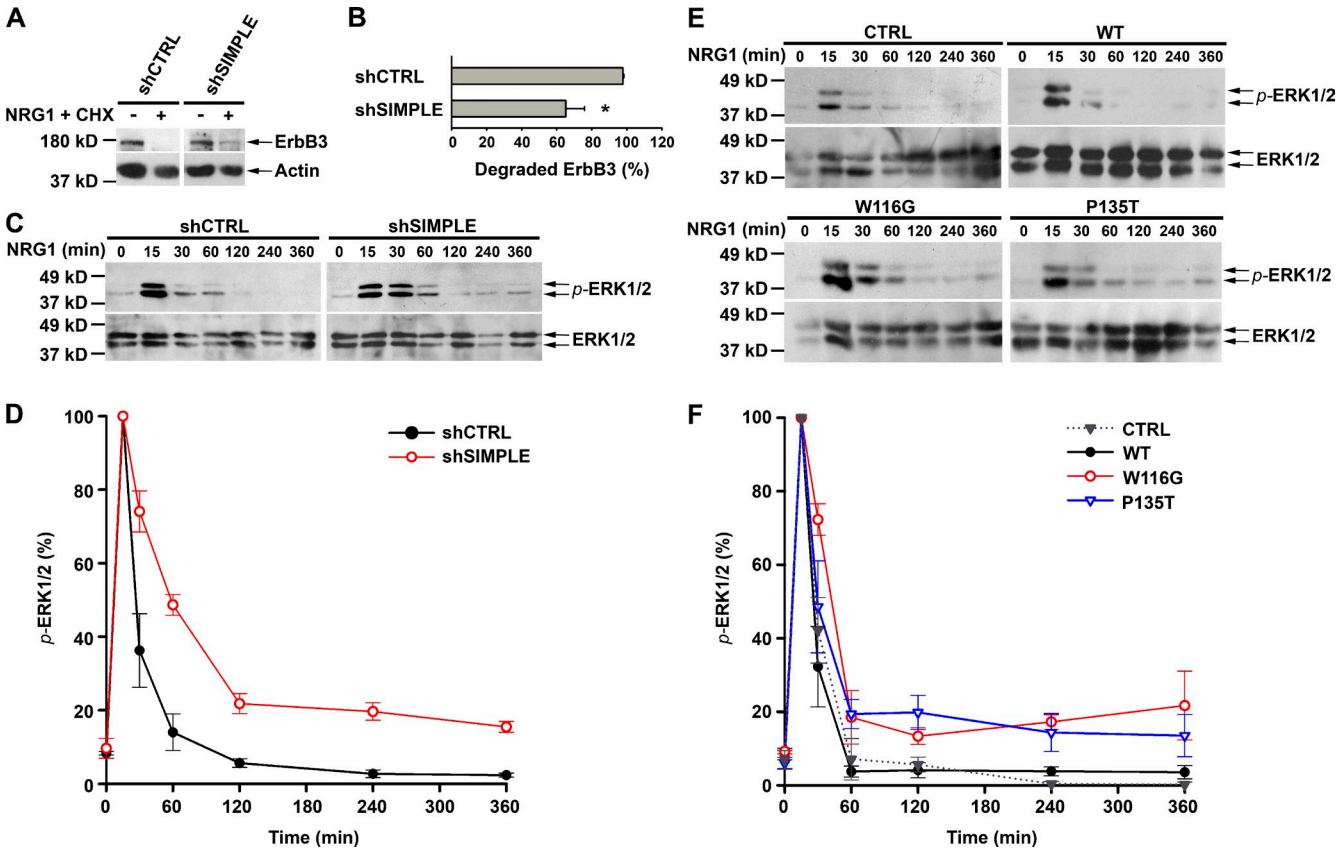

Figure 10. **CMT1C-linked SIMPLE mutants have dominant-negative effects on NRG1-ErbB signaling in Schwann cells.** (A and B) Mouse MSC80 Schwann cells stably transfected with the indicated shRNAs were incubated in the absence or presence of 10 nM NRG1 and 100 µg/ml cycloheximide (CHX) for 4 h. ErbB3 degradation analysis (A) and quantification (B) show reduced levels of NRG1-induced ErbB3 degradation in shSIMPLE-transfected Schwann cells compared with the shCTRL-transfected control. Data represent mean ± SEM (error bars; $n = 3$). *, $P < 0.05$, unpaired two-tailed Student's t test. (C and D) Immunoblot analysis (C) and quantification (D) show levels of *p*-ERK1/2 and total ERK1/2 at the indicated times after treatment with 10 nM NRG1 in shSIMPLE- or shCTRL-transfected Schwann cells. The *p*-ERK1/2 level was normalized to the ERK1/2 level and plotted as a percentage of the peak value of the normalized *p*-ERK1/2 level. Data represent mean ± SEM (error bars; $n = 3$). (E and F) Immunoblot analysis (E) and quantification (F) show levels of *p*-ERK1/2 and total ERK1/2 at the indicated times after treatment with 10 nM NRG1 in MSC80 cells expressing the indicated Myc-tagged SIMPLE WT or mutant, or Myc vector (CTRL). The *p*-ERK1/2 level was normalized to the ERK1/2 level and plotted as a percentage of the peak value of the normalized *p*-ERK1/2 level. Data represent mean ± SEM (error bars; $n = 3$).

CMT. We have shown that SIMPLE is a ubiquitously expressed protein with high abundance in Schwann cells (Lee et al., 2011). The fact that SIMPLE mutations cause demyelinating peripheral neuropathy in human CMT1C patients suggests that, compared with other cell types, Schwann cells are particularly vulnerable to defects in endosomal trafficking. Consistent with this notion, mutations in several ubiquitously expressed regulators of endosome-to-lysosome trafficking, such as MTMR2 (Cao et al., 2008), MTMR13 (Bolis et al., 2007), and FIG4 (Rutherford et al., 2006), have been identified as the genetic defects for causing demyelinating forms of CMT (Bolino et al., 2000; Senderek et al., 2003; Chow et al., 2007). Thus, dysregulation of endosome-to-lysosome trafficking may be a common pathogenic mechanism in several demyelinating CMT diseases. Our analyses reveal that SIMPLE plays an essential role in the regulation of NRG1-induced ErbB degradation and signaling attenuation in Schwann cells. Furthermore, SIMPLE mutations cause dysregulation of NRG1-ErbB signaling, leading to prolonged ERK1/2 activation. These results, together with the reports that persistent ERK1/2 activation leads to demyelination (Ogata et al., 2004; Nave and Salzer, 2006; Quintes et al., 2010; Syed et al., 2010), suggest a pathogenic pathway by which SIMPLE mutations cause dysregulated NRG1-ErbB signaling in Schwann cells and thereby trigger demyelination and subsequent axonal degeneration, leading to peripheral neuropathy. In conclusion, our findings obtained from this work have filled a critical gap in our knowledge about the function of SIMPLE in cells, and have provided new insights into the pathogenic mechanism of CMT1C-linked SIMPLE mutations in peripheral neuropathy.

Materials and methods

Plasmids

The cDNAs encoding human SIMPLE WT, CMT1C-linked mutants, and SIMPLE deletion mutants were generated by conventional molecular biological techniques, and were confirmed by DNA sequencing. Each cDNA was then subcloned into expression vectors that add an N-terminal Myc, HA, GFP, GST, or His×6 tags. The rescue expression vectors encoding SIMPLE-targeting shRNA-resistant, epitope-tagged SIMPLE WT, W116G, P135T, and ASAA mutants were generated by site-directed mutagenesis to make two or more silent third-codon substitutions within the shRNA-targeted region of the SIMPLE transcript without altering the amino acid sequence of the SIMPLE protein. N-terminal HA-tagged NEDD4 and Myc-tagged NEDD4 expression constructs were provided by A. Weissman

(National Institutes of Health, Bethesda, MD) and B. Whatley (Emory University, Atlanta, GA), respectively. N-terminal HA-tagged STAM1 and His-tagged STAM1 expression constructs were provided by M. Komada (Tokyo Institute of Technology, Tokyo, Japan) and V. Tangpisuthipongsa (Emory University), respectively, and were used to generate an N-terminal GFP-tagged STAM1 expression construct by conventional molecular biological techniques. ShRNA constructs targeting human SIMPLE (Public TRC Portal no. NM_004862.1-397s1c1 and NM_004862.1-291s1c1; Sigma-Aldrich) and mouse SIMPLE (Public TRC Portal no. NM_019980.1-269s1c1 and NM_019980.1-881s21c1; Sigma-Aldrich) and nontargeting shRNA control construct (SHC001; Sigma-Aldrich) were obtained commercially.

Antibodies
Polyclonal antibodies were generated against synthetic peptides corresponding to amino acid residues 50–64 of human SIMPLE (anti-SIMPLE antibody), 316–335 of human STAM1 (anti-STAM1 antibody), 758–771 of rat Hrs (anti-Hrs antibody), or 171–189 of human DJ-1 (anti–DJ-1 antibody). The antibodies were affinity purified using the immunogen peptides coupled to a SulfoLink column (Thermo Fisher Scientific) according to the manufacturer's instructions. Other antibodies used in this study include the following: anti-GFP (Santa Cruz Biotechnology, Inc.), GST (Santa Cruz Biotechnology, Inc.), Myc (9E10), HA (12CA5 and 3F10; Roche), TSG101 (GeneTex), EEA1 (BD), LAMP2 (Iowa Developmental Studies Hybridoma Bank), anti-EGFR (Santa Cruz Biotechnology, Inc.), ErbB3 (Abgent), ERK1/2 (Cell Signaling Technology), phospho-ERK1/2 (Cell Signaling Technology), phospho-tyrosine (Cell Signaling Technology), and Actin (Sigma-Aldrich). All secondary antibodies were purchased from Jackson ImmunoResearch Laboratories, Inc.

Yeast two-hybrid screens
Full-length human SIMPLE was subcloned into the pPC97 vector to generate the bait plasmid pPC97-SIMPLE. The rat hippocampal/cortical two-hybrid cDNA library was provided by P. Worley (Johns Hopkins University, Baltimore, MD). Yeast two-hybrid screens this cDNA library were performed in yeast strain CG-1945 (Takara Bio Inc.) transformed with pPC97-SIMPLE. Positive prey clones encoding SIMPLE-binding proteins were selected by growth on a medium containing 5 mM 3-aminotriazole (Sigma-Aldrich) but lacking leucine, tryptophan, and histidine. The bait–prey interactions were validated by using a filter assay of β-galactosidase activity. The specificity of the identified interactions were confirmed by retransformation of isolated prey plasmids into fresh yeast cells with either the pPC97-SIMPLE plasmid or control bait plasmids.

Immunoblot analyses
Protein extracts were prepared by homogenizing cells in 1% SDS and then subjected to SDS-PAGE. The separated proteins were transferred onto nitrocellulose membranes and probed with the indicated antibodies against STAM1 (1:5,000), GST (1:5,000), Myc (9E10, 1:10,000), HA (12CA5, 1:100,000; 3F10, 1:1,000), Hrs (1:10,000), SIMPLE (1:5,000), EGFR (1:1,000), Actin (1:3,000), ERK1/2 (1:1,000), phospho-ERK1/2 (1:1,000), TSG101 (1:1,000), LAMP2 (1:1,000), DJ-1 (1:100,000), phospho-tyrosine (1:1,000), GFP (1:1,000), or ErbB3 (1:1,000). Antibody binding was detected using the ECL system (GE Healthcare). The immunoblot images were scanned at 600 dpi with ScanMaker, using the Scanwizard software (Microtek). Photoshop CS3 software (Adobe) was used to adjust the brightness and to generate the figures.

Recombinant protein purification, in vitro binding assays, and GST pull-down assays
His-tagged STAM1 and SIMPLE, GST-tagged SIMPLE full-length WT, deletion; and CMT1C-linked mutants, Hrs, STAM1, and GST proteins were individually expressed in *Escherichia coli* BL21 or ArcticExpress competent cells (Agilent Technologies) and purified by affinity chromatography using the glutathione-agarose beads (Sigma-Aldrich) for GST-tagged proteins or Ni-NTA-agarose beads (QIAGEN) for His-tagged proteins. In vitro binding assays were performed as described previously (Li et al., 2001) by incubation of immobilized GST-tagged proteins or GST with purified proteins for 2 h at 4°C under gentle rocking in 50 mM Tris-HCl, pH 8.0, 150 mM NaCl, and 0.1% Triton-X100. GST pull-down assays were performed as described previously (Li et al., 2001) by incubation of immobilized GST-tagged proteins or GST with lysates of transfected HeLa cells as indicated for 2 h at 4°C. Bound proteins were analyzed by SDS-PAGE and immunoblot analyses.

In vitro ubiquitination assays
In vitro ubiquitination assays were performed using a well-established reconstitution system as described previously (Kim et al., 2007; Shimura et al., 2000). In brief, GST-tagged parkin or SIMPLE protein was incubated at 37°C in 100 µl reaction buffer (50 mM Tris-HCL, pH 7.4, 5 mM $MgCl_2$, 0.6 mM dithiothreitol, and 2 mM ATP) containing 10 µg of ubiquitin, 200 ng of recombinant E1, and 400 ng of recombinant E2 as indicated in the presence and absence of His-tagged STAM1 or immunopurified GFP-tagged TSG101. After incubation for 2 h at 37°C, the reaction products were analyzed by SDS-PAGE and immunoblotting.

Cell transfections and immunoprecipitation
Mouse MSC80 Schwann cells (Boutry et al., 1992) were provided by R. Chrast (University of Lausanne, Lausanne, Switzerland) and J.-Y. Cesbron (Université Joseph Fourier, Grenoble, France). MSC80 cells or HeLa cells were transfected with the indicated plasmids using Lipofectamine 2000 (Invitrogen) in accordance to the manufacturer's instructions. Stably transfected cells were selected using 1 mg/ml G418 (Sigma-Aldrich) or 2.5 µg/ml puromycin (Research Products International). For immunoprecipitations, cells were homogenized in lysis buffer (50 mM Tris-HCl, pH 7.6, 100 mM NaCl, 1% IGEPAL, 0.1% Triton X-100, and a cocktail of protease inhibitors), and cell lysates were incubated with anti-SIMPLE (rabbit polyclonal), anti-HA (12CA5), or anti-Myc (9E10) antibodies for 4 h at 4°C. Immunocomplexes were recovered by protein G–Sepharose beads (EMD Millipore). After extensive washes, immunocomplexes were boiled in the Laemmli sample buffer and were analyzed by SDS-PAGE and immunoblotting.

Subcellular fractionation
HeLa cells expressing the indicated shRNAs or exogenous proteins were treated with 100 ng/ml EGF for 15 min or left untreated. Cells were then subjected to subcellular fractionation as described previously (Lee et al., 2011). In brief, cells were homogenized in 1 ml of homogenization buffer (250 mM sucrose, 10 mM HEPES/KOH, pH 7.4, 10 mM KCl, 10 mM EGTA, and 0.1 mM EDTA) containing protease inhibitors and dithiothreitol. After centrifugation at 1,000 *g* to remove unbroken cells and nuclei, the postnuclear supernatants were subjected to a 30-min centrifugation at 100,000 *g* to separate into membrane (pellet) and cytosol (supernatant) fractions. Aliquots representing an equal percentage of each fraction were analyzed by SDS-PAGE and immunoblot analyses.

Immunofluorescence confocal microscopy
Cells were fixed in 4% paraformaldehyde with PBS and were processed as described previously (Olzmann et al., 2007). In brief, cells were fixed with 4% paraformaldehyde in 1× PBS for 10 min, permeabilized with a solution containing 0.1% saponin (Sigma-Aldrich) and 10% horse serum in 1× PBS, stained with the indicated primary antibodies followed by secondary antibodies conjugated to FITC, Texas red, or Cy5, and then mounted in ProLong Gold antifade reagent with DAPI as directed by the manufacturer (Invitrogen). For immunofluorescence confocal microscopic analyses, cell images were acquired in room temperature with a confocal microscope (Eclipse Ti; Nikon) equipped with Plan-Apochromat 40×/1.3 NA or 60×/1.4 NA oil immersion objective lenses; filter sets for FITC, TRITC, DAPI, and DIC; a DS-Qi1 camera (Nikon); and the EZ-C1 acquisition software (Nikon). For oil immersion, type A immersion oil (Nikon) was used. The acquired 16-bit RGB images were converted into 8-bit RGB images with the EZ-C1 acquisition software (Nikon), and Photoshop CS3 software was used to adjust the brightness and to produce the figures. Cell images in Fig. S2 (C and D) were acquired with the laser scanning confocal microscope (LSM 510; Carl Zeiss) equipped with a Plan-Apochromat 63×/1.4 NA oil immersion objective lens (used with Immersol 518 immersion oil; Carl Zeiss); filter sets for FITC, Rhodamine, DAPI, and DIC; a camera (AxioCam; Carl Zeiss); and the LSM 510 operating software (Carl Zeiss). The acquired 8-bit RGB images were exported to TIFF files with the LSM510 viewer software (Carl Zeiss), and Photoshop CS3 software was used to adjust the brightness and to produce the figures.

3D-SIM
For 3D-SIM analysis, cells were fixed and stained as described in the preceding paragraph for immunofluorescence confocal microscopy. Cell images were acquired at room temperature with a microscope (N-SIM; Nikon) equipped with an Apochromat total internal reflection fluorescence 100×/1.49 NA oil immersion objective lens, an EM charge-coupled device (CCD) camera (DU-897; Nikon), the 488 nm and 561 nm laser lines, and the NIS-Elements software with workstation (Nikon). For oil immersion, a type NF immersion oil lens (Nikon) was used. Image stacks with z height up to 10 µm and a z distance of 500 nm were acquired. For each z plane of the cell, 15 images of the green (FITC) fluorescence were acquired with a different illumination pattern (5 phases and 3 angles), and these

15 images were computationally reconstructed by NIS-Elements software with workstation (Nikon) to generate a super-resolution image with twofold enhanced resolution in all three axes. For the imaging of DAPI staining, conventional wide-field images were acquired for each z plane of the cell. The acquired 16-bit RGB images were converted into 8-bit RGB images with the NIS-Elements software (Nikon), and Photoshop CS3 software was used to adjust the brightness and to produce the figures.

Quantification of colocalization, endosome size, and dispersion

For quantification, all images from a given experiment were acquired with the identical settings from the same microscope. Quantification of the colocalization of SIMPLE with various marker proteins was performed on unprocessed images. Single cells were selected by manually tracing the cell outlines. The background was subtracted and the percentage of SIMPLE overlapping with various markers and the percentage of various markers overlapping SIMPLE were determined by Mander's coefficients via the ImageJ software with the JACOP plugin (Bolte and Cordelières, 2006; Rodal et al., 2011). The percentages of overlap were averaged from a total of 25–40 randomly selected cells per group. The diameters and areas of EEA1-positive endosomes were quantified from unprocessed images using NIS-Elements software (Nikon). Diameters and areas of endosomes were averaged for each cell from a total of 30–40 randomly selected cells in each group. The quantification of endosome dispersion was performed as described previously (Tuma et al., 1998). In brief, distances between the coordinates of each endosome from the center of mass were quantified using NIS-Elements software and averaged for each cell. A total of 40–50 randomly selected cells were analyzed per group, and the mean endosomal distance was normalized to the control. Graphs were generated with SigmaPlot 11.0 software (Systat Software, Inc.), and Photoshop CS3 software was used to produce the figures.

EGF endocytic trafficking assays

TR-EGF endocytosis assays were performed as described previously (Kirk et al., 2006; Webber et al., 2008). In brief, HeLa cells transfected with the indicated constructs were incubated in serum-free media for 4 h, and then treated with 3 µg/ml TR-EGF (Invitrogen) in the presence of 0.1% BSA at 37°C for 15 min followed by immunofluorescence confocal microscopic analysis. TR-EGF endosome-to-lysosome trafficking analysis was performed as described previously (Kirk et al., 2006; Webber et al., 2008). In brief, cells were first allowed to internalize TR-EGF for 15 min. After washing three times with the media to remove extracellular TR-EGF, cells were incubated for an additional 1 h at 37°C and then processed for immunofluorescence confocal microscopy. Quantification of the amount of intracellular TR-EGF was performed on unprocessed images. ImageJ software (National Institutes of Health) was used to integrate the pixel intensity above background for 50–100 cells in each group from three separate experiments.

EGFR and ErbB3 degradation assays

For EGFR degradation assays, HeLa cells transfected with the indicated constructs were serum starved for 18 h and then incubated in the presence or absence of 100 ng/ml EGF (Invitrogen) for 1 h at 37°C. Equal amounts of protein from whole cell lysates were analyzed by immunoblotting. The EGFR levels were quantified by measuring the intensity of the EGFR bands on immunoblot images using the National Institutes of Health Image/Scion software. The degraded EGFR induced by EGF treatment is expressed as a percentage of the EGFR level of corresponding untreated cells. For ErbB3 degradation assays, MSC80 cells transfected with the indicated constructs were serum starved for 18 h and then incubated in the absence or presence of 10 nM NRG1 (R&D Systems) and 100 µg/ml of cycloheximide (Sigma-Aldrich) for 4 h at 37°C. The cells were lysed in 1% SDS, and an equal amount of protein from each lysate was then subjected to immunoblot analyses. The ErbB3 levels were quantified from immunoblot images using the NIH Image/Scion software. The degraded ErbB3 induced by NRG1 treatment is expressed as a percentage of the ErbB3 level of corresponding untreated cells.

SIMPLE tyrosine phosphorylation assays

HeLa cells were starved for 18 h and then incubated in the presence or absence of 100 ng/ml EGF (Invitrogen) for 15 min at 37°C. Cells were lysed in the presence of 100 µM sodium orthovanadate and subjected to immunoprecipitation with anti-SIMPLE antibody or control rabbit IgG. Tyrosine phosphorylation of immunoprecipitated SIMPLE was detected by immunoblot analysis using anti–phospho-tyrosine and anti-SIMPLE antibodies.

ERK1/2 phosphorylation assays

HeLa or MSC80 cells transfected with the indicated constructs were starved in serum-free medium for 18 h and then treated with 10 ng/ml EGF or 10 nM NRG-1, respectively, for the indicated times at 37°C, as described previously (Xu et al., 2012). After treatment, cells were lysed in 1% SDS. An equal amount of protein from each lysate was subjected to immunoblot analysis using anti-phospho-ERK1/2 and anti-ERK1/2 antibodies.

Statistical analysis

Data were subjected to statistical analyses by a Student's *t* test or one- or two-way analysis of variance with a Tukey's post hoc test using the SigmaPlot software. Results are expressed as mean ± SEM. A p-value of <0.05 was considered statistically significant.

Online supplemental material

Fig. S1 shows that SIMPLE interacts indirectly with Hrs and associates with ESCRT subunits at the early endosomes. Fig. S2 shows that SIMPLE has no E3 ligase activity and does not interact with E2 enzymes UbcH5, UbcH7, and UbcH8. Fig. S3 shows that the depletion of SIMPLE has no effect on the stability of STAM1 or Hrs. Fig. S4 shows that overexpression of Hrs does not rescue the SIMPLE depletion phenotype and vice versa. Fig. S5 shows the analyses of endogenous and exogenous SIMPLE protein expression in stably transfected HeLa and MSC80 cells. Online supplemental material is available at http://www.jcb.org/cgi/content/full/jcb.201204137/DC1.

We thank Yifei Pu for assistance with yeast two-hybrid screens and James Olzmann for the SIMPLE–TSG101 colocalization analysis.

This work was supported by the National Institutes of Health (NIH; NS063501 to S.M. Lee, AG034126 to L.-S. Chin, ES015813 and GM082828 to L. Li) and the Emory University Research Committee (SK38167 to L.-S. Chin). We thank Emory Neuroscience Imaging Core Facility (supported in part by NIH grant NS055077) for providing instrumentation and support.

Submitted: 26 April 2012
Accepted: 25 October 2012

References

Babst, M., G. Odorizzi, E.J. Estepa, and S.D. Emr. 2000. Mammalian tumor susceptibility gene 101 (TSG101) and the yeast homologue, Vps23p, both function in late endosomal trafficking. *Traffic*. 1:248–258. http://dx.doi.org/10.1034/j.1600-0854.2000.010307.x

Bache, K.G., A. Brech, A. Mehlum, and H. Stenmark. 2003a. Hrs regulates multivesicular body formation via ESCRT recruitment to endosomes. *J. Cell Biol.* 162:435–442. http://dx.doi.org/10.1083/jcb.200302131

Bache, K.G., C. Raiborg, A. Mehlum, and H. Stenmark. 2003b. STAM and Hrs are subunits of a multivalent ubiquitin-binding complex on early endosomes. *J. Biol. Chem.* 278:12513–12521. http://dx.doi.org/10.1074/jbc.M210843200

Bache, K.G., T. Slagsvold, A. Cabezas, K.R. Rosendal, C. Raiborg, and H. Stenmark. 2004. The growth-regulatory protein HCRP1/hVps37A is a subunit of mammalian ESCRT-I and mediates receptor down-regulation. *Mol. Biol. Cell*. 15:4337–4346. http://dx.doi.org/10.1091/mbc.E04-03-0250

Birchmeier, C. 2009. ErbB receptors and the development of the nervous system. *Exp. Cell Res.* 315:611–618. http://dx.doi.org/10.1016/j.yexcr.2008.10.035

Bolino, A., M. Muglia, F.L. Conforti, E. LeGuern, M.A. Salih, D.M. Georgiou, K. Christodoulou, I. Hausmanowa-Petrusewicz, P. Mandich, A. Schenone, et al. 2000. Charcot-Marie-Tooth type 4B is caused by mutations in the gene encoding myotubularin-related protein-2. *Nat. Genet.* 25:17–19. http://dx.doi.org/10.1038/75542

Bolis, A., P. Zordan, S. Coviello, and A. Bolino. 2007. Myotubularin-related (MTMR) phospholipid phosphatase proteins in the peripheral nervous system. *Mol. Neurobiol.* 35:308–316. http://dx.doi.org/10.1007/s12035-007-0031-0

Bolte, S., and F.P. Cordelières. 2006. A guided tour into subcellular colocalization analysis in light microscopy. *J. Microsc.* 224:213–232. http://dx.doi.org/10.1111/j.1365-2818.2006.01706.x

Boutry, J.M., J.J. Hauw, A. Gansmüller, N. Di-Bert, M. Pouchelet, and A. Baron-Van Evercooren. 1992. Establishment and characterization of a mouse Schwann cell line which produces myelin in vivo. *J. Neurosci. Res.* 32:15–26. http://dx.doi.org/10.1002/jnr.490320103

Campbell, R., H. Dorey, M. Naegeli, L.K. Grubstein, K.K. Bennett, F. Bonter, P.K. Smith, J. Grzywacz, P.K. Baker, and W.S. Davidson. 2004. An empowerment evaluation model for sexual assault programs: empirical evidence of effectiveness. *Am. J. Community Psychol.* 34:251–262. http://dx.doi.org/10.1007/s10464-004-7418-0

Cao, Z., X. Wu, L. Yen, C. Sweeney, and K.L. Carraway III. 2007. Neuregulin-induced ErbB3 downregulation is mediated by a protein stability cascade involving the E3 ubiquitin ligase Nrdp1. *Mol. Cell. Biol.* 27:2180–2188. http://dx.doi.org/10.1128/MCB.01245-06

Cao, C., J.M. Backer, J. Laporte, E.J. Bedrick, and A. Wandinger-Ness. 2008. Sequential actions of myotubularin lipid phosphatases regulate endosomal PI(3)P and growth factor receptor trafficking. *Mol. Biol. Cell*. 19:3334–3346. http://dx.doi.org/10.1091/mbc.E08-04-0367

Chen, S., M.O. Velardez, X. Warot, Z.X. Yu, S.J. Miller, D. Cros, and G. Corfas. 2006. Neuregulin 1-erbB signaling is necessary for normal myelination and sensory function. *J. Neurosci.* 26:3079–3086. http://dx.doi.org/10.1523/JNEUROSCI.3785-05.2006

Chin, L.S., M.C. Raynor, X.L. Wei, H.Q. Chen, and L. Li. 2001. Hrs interacts with sorting nexin 1 and regulates degradation of epidermal growth factor receptor. *J. Biol. Chem.* 276:7069–7078. http://dx.doi.org/10.1074/jbc.M004129200

Chow, C.Y., Y. Zhang, J.J. Dowling, N. Jin, M. Adamska, K. Shiga, K. Szigeti, M.E. Shy, J. Li, X. Zhang, et al. 2007. Mutation of FIG4 causes neurodegeneration in the pale tremor mouse and patients with CMT4J. *Nature*. 448:68–72. http://dx.doi.org/10.1038/nature05876

Doyotte, A., M.R. Russell, C.R. Hopkins, and P.G. Woodman. 2005. Depletion of TSG101 forms a mammalian "Class E" compartment: a multicisternal early endosome with multiple sorting defects. *J. Cell Sci.* 118:3003–3017. http://dx.doi.org/10.1242/jcs.02421

Gerding, W.M., J. Koetting, J.T. Epplen, and C. Neusch. 2009. Hereditary motor and sensory neuropathy caused by a novel mutation in LITAF. *Neuromuscul. Disord.* 19:701–703. http://dx.doi.org/10.1016/j.nmd.2009.05.006

Gillooly, D.J., C. Raiborg, and H. Stenmark. 2003. Phosphatidylinositol 3-phosphate is found in microdomains of early endosomes. *Histochem. Cell Biol.* 120:445–453. http://dx.doi.org/10.1007/s00418-003-0591-7

Henne, W.M., N.J. Buchkovich, and S.D. Emr. 2011. The ESCRT pathway. *Dev. Cell*. 21:77–91. http://dx.doi.org/10.1016/j.devcel.2011.05.015

Huang, B., M. Bates, and X. Zhuang. 2009. Super-resolution fluorescence microscopy. *Annu. Rev. Biochem.* 78:993–1016. http://dx.doi.org/10.1146/annurev.biochem.77.061906.092014

Kanazawa, C., E. Morita, M. Yamada, N. Ishii, S. Miura, H. Asao, T. Yoshimori, and K. Sugamura. 2003. Effects of deficiencies of STAMs and Hrs, mammalian class E Vps proteins, on receptor downregulation. *Biochem. Biophys. Res. Commun.* 309:848–856. http://dx.doi.org/10.1016/j.bbrc.2003.08.078

Katzmann, D.J., G. Odorizzi, and S.D. Emr. 2002. Receptor downregulation and multivesicular-body sorting. *Nat. Rev. Mol. Cell Biol.* 3:893–905. http://dx.doi.org/10.1038/nrm973

Kim, B.Y., J.A. Olzmann, G.S. Barsh, L.S. Chin, and L. Li. 2007. Spongiform neurodegeneration-associated E3 ligase Mahogunin ubiquitylates TSG101 and regulates endosomal trafficking. *Mol. Biol. Cell*. 18:1129–1142. http://dx.doi.org/10.1091/mbc.E06-09-0787

Kirk, E., L.S. Chin, and L. Li. 2006. GRIF1 binds Hrs and is a new regulator of endosomal trafficking. *J. Cell Sci.* 119:4689–4701. http://dx.doi.org/10.1242/jcs.03249

Latour, P., P.M. Gonnaud, E. Ollagnon, V. Chan, S. Perelman, T. Stojkovic, C. Stoll, C. Vial, F. Ziegler, A. Vandenberghe, and I. Maire. 2006. SIMPLE mutation analysis in dominant demyelinating Charcot-Marie-Tooth disease: three novel mutations. *J. Peripher. Nerv. Syst.* 11:148–155. http://dx.doi.org/10.1111/j.1085-9489.2006.00080.x

Lee, S.M., J.A. Olzmann, L.S. Chin, and L. Li. 2011. Mutations associated with Charcot-Marie-Tooth disease cause SIMPLE protein mislocalization and degradation by the proteasome and aggresome-autophagy pathways. *J. Cell Sci.* 124:3319–3331. http://dx.doi.org/10.1242/jcs.087114

Li, Y., L.S. Chin, C. Weigel, and L. Li. 2001. Spring, a novel RING finger protein that regulates synaptic vesicle exocytosis. *J. Biol. Chem.* 276:40824–40833. http://dx.doi.org/10.1074/jbc.M106141200

Li, Y., L.S. Chin, A.I. Levey, and L. Li. 2002. Huntingtin-associated protein 1 interacts with hepatocyte growth factor-regulated tyrosine kinase substrate and functions in endosomal trafficking. *J. Biol. Chem.* 277:28212–28221. http://dx.doi.org/10.1074/jbc.M111612200

Martyn, C.N., and R.A. Hughes. 1997. Epidemiology of peripheral neuropathy. *J. Neurol. Neurosurg. Psychiatry*. 62:310–318. http://dx.doi.org/10.1136/jnnp.62.4.310

Mellman, I. 1996a. Endocytosis and molecular sorting. *Annu. Rev. Cell Dev. Biol.* 12:575–625. http://dx.doi.org/10.1146/annurev.cellbio.12.1.575

Mellman, I. 1996b. Membranes and sorting. *Curr. Opin. Cell Biol.* 8:497–498. http://dx.doi.org/10.1016/S0955-0674(96)80026-3

Mizuno, E., K. Kawahata, A. Okamoto, N. Kitamura, and M. Komada. 2004. Association with Hrs is required for the early endosomal localization, stability, and function of STAM. *J. Biochem.* 135:385–396. http://dx.doi.org/10.1093/jb/mvh046

Morino, C., M. Kato, A. Yamamoto, E. Mizuno, A. Hayakawa, M. Komada, and N. Kitamura. 2004. A role for Hrs in endosomal sorting of ligand-stimulated and unstimulated epidermal growth factor receptor. *Exp. Cell Res.* 297:380–391. http://dx.doi.org/10.1016/j.yexcr.2004.03.038

Moriwaki, Y., N.A. Begum, M. Kobayashi, M. Matsumoto, K. Toyoshima, and T. Seya. 2001. *Mycobacterium bovis* Bacillus Calmette-Guerin and its cell wall complex induce a novel lysosomal membrane protein, SIMPLE, that bridges the missing link between lipopolysaccharide and p53-inducible gene, LITAF(PIG7), and estrogen-inducible gene, EET-1. *J. Biol. Chem.* 276:23065–23076. http://dx.doi.org/10.1074/jbc.M011660200

Nave, K.A., and J.L. Salzer. 2006. Axonal regulation of myelination by neuregulin 1. *Curr. Opin. Neurobiol.* 16:492–500. http://dx.doi.org/10.1016/j.conb.2006.08.008

Newbern, J., and C. Birchmeier. 2010. Nrg1/ErbB signaling networks in Schwann cell development and myelination. *Semin. Cell Dev. Biol.* 21:922–928. http://dx.doi.org/10.1016/j.semcdb.2010.08.008

Ogata, T., S. Iijima, S. Hoshikawa, T. Miura, S. Yamamoto, H. Oda, K. Nakamura, and S. Tanaka. 2004. Opposing extracellular signal-regulated kinase and Akt pathways control Schwann cell myelination. *J. Neurosci.* 24:6724–6732. http://dx.doi.org/10.1523/JNEUROSCI.5520-03.2004

Olzmann, J.A., L. Li, M.V. Chudaev, J. Chen, F.A. Perez, R.D. Palmiter, and L.S. Chin. 2007. Parkin-mediated K63-linked polyubiquitination targets misfolded DJ-1 to aggresomes via binding to HDAC6. *J. Cell Biol.* 178:1025–1038. http://dx.doi.org/10.1083/jcb.200611128

Parman, Y. 2007. Hereditary neuropathies. *Curr. Opin. Neurol.* 20:542–547. http://dx.doi.org/10.1097/WCO.0b013e32826fbcb7

Pornillos, O., S.L. Alam, R.L. Rich, D.G. Myszka, D.R. Davis, and W.I. Sundquist. 2002. Structure and functional interactions of the Tsg101 UEV domain. *EMBO J.* 21:2397–2406. http://dx.doi.org/10.1093/emboj/21.10.2397

Quintes, S., S. Goebbels, G. Saher, M.H. Schwab, and K.A. Nave. 2010. Neuron-glia signaling and the protection of axon function by Schwann cells. *J. Peripher. Nerv. Syst.* 15:10–16. http://dx.doi.org/10.1111/j.1529-8027.2010.00247.x

Raiborg, C., K.G. Bache, A. Mehlum, E. Stang, and H. Stenmark. 2001. Hrs recruits clathrin to early endosomes. *EMBO J.* 20:5008–5021. http://dx.doi.org/10.1093/emboj/20.17.5008

Razi, M., and C.E. Futter. 2006. Distinct roles for Tsg101 and Hrs in multivesicular body formation and inward vesiculation. *Mol. Biol. Cell*. 17:3469–3483. http://dx.doi.org/10.1091/mbc.E05-11-1054

Rodal, A.A., A.D. Blunk, Y. Akbergenova, R.A. Jorquera, L.K. Buhl, and J.T. Littleton. 2011. A presynaptic endosomal trafficking pathway controls synaptic growth signaling. *J. Cell Biol.* 193:201–217. http://dx.doi.org/10.1083/jcb.201009052

Roxrud, I., H. Stenmark, and L. Malerød. 2010. ESCRT & Co. *Biol. Cell*. 102:293–318. http://dx.doi.org/10.1042/BC20090161

Rutherford, A.C., C. Traer, T. Wassmer, K. Pattni, M.V. Bujny, J.G. Carlton, H. Stenmark, and P.J. Cullen. 2006. The mammalian phosphatidylinositol 3-phosphate 5-kinase (PIKfyve) regulates endosome-to-TGN retrograde transport. *J. Cell Sci.* 119:3944–3957. http://dx.doi.org/10.1242/jcs.03153

Saifi, G.M., K. Szigeti, W. Wiszniewski, M.E. Shy, K. Krajewski, I. Hausmanowa-Petrusewicz, A. Kochanski, S. Reeser, P. Mancias, I. Butler, and J.R. Lupski. 2005. SIMPLE mutations in Charcot-Marie-Tooth disease and the potential role of its protein product in protein degradation. *Hum. Mutat.* 25:372–383. http://dx.doi.org/10.1002/humu.20153

Schermelleh, L., P.M. Carlton, S. Haase, L. Shao, L. Winoto, P. Kner, B. Burke, M.C. Cardoso, D.A. Agard, M.G. Gustafsson, et al. 2008. Subdiffraction multicolor imaging of the nuclear periphery with 3D structured illumination microscopy. *Science*. 320:1332–1336. http://dx.doi.org/10.1126/science.1156947

Senderek, J., C. Bergmann, S. Weber, U.P. Ketelsen, H. Schorle, S. Rudnik-Schöneborn, R. Büttner, E. Buchheim, and K. Zerres. 2003. Mutation of the SBF2 gene, encoding a novel member of the myotubularin family, in Charcot-Marie-Tooth neuropathy type 4B2/11p15. *Hum. Mol. Genet.* 12:349–356. http://dx.doi.org/10.1093/hmg/ddg030

Shimura, H., N. Hattori, S. Kubo, Y. Mizuno, S. Asakawa, S. Minoshima, N. Shimizu, K. Iwai, T. Chiba, K. Tanaka, and T. Suzuki. 2000. Familial Parkinson disease gene product, parkin, is a ubiquitin-protein ligase. *Nat. Genet.* 25:302–305. http://dx.doi.org/10.1038/77060

Shirk, A.J., S.K. Anderson, S.H. Hashemi, P.F. Chance, and C.L. Bennett. 2005. SIMPLE interacts with NEDD4 and TSG101: evidence for a role in lysosomal sorting and implications for Charcot-Marie-Tooth disease. *J. Neurosci. Res.* 82:43–50. http://dx.doi.org/10.1002/jnr.20628

Sorkin, A., and L.K. Goh. 2009. Endocytosis and intracellular trafficking of ErbBs. *Exp. Cell Res.* 315:683–696. http://dx.doi.org/10.1016/j.yexcr.2008.07.029

Street, V.A., C.L. Bennett, J.D. Goldy, A.J. Shirk, K.A. Kleopa, B.L. Tempel, H.P. Lipe, S.S. Scherer, T.D. Bird, and P.F. Chance. 2003. Mutation of a putative protein degradation gene LITAF/SIMPLE in Charcot-Marie-Tooth disease 1C. *Neurology*. 60:22–26. http://dx.doi.org/10.1212/WNL.60.1.22

Syed, N., K. Reddy, D.P. Yang, C. Taveggia, J.L. Salzer, P. Maurel, and H.A. Kim. 2010. Soluble neuregulin-1 has bifunctional, concentration-dependent effects on Schwann cell myelination. *J. Neurosci.* 30:6122–6131. http://dx.doi.org/10.1523/JNEUROSCI.1681-09.2010

Tuma, M.C., A. Zill, N. Le Bot, I. Vernos, and V. Gelfand. 1998. Heterotrimeric kinesin II is the microtubule motor protein responsible for pigment dispersion in Xenopus melanophores. *J. Cell Biol.* 143:1547–1558. http://dx.doi.org/10.1083/jcb.143.6.1547

Urbé, S., M. Sachse, P.E. Row, C. Preisinger, F.A. Barr, G. Strous, J. Klumperman, and M.J. Clague. 2003. The UIM domain of Hrs couples receptor sorting to vesicle formation. *J. Cell Sci.* 116:4169–4179. http://dx.doi.org/10.1242/jcs.00723

Waterman, H., and Y. Yarden. 2001. Molecular mechanisms underlying endocytosis and sorting of ErbB receptor tyrosine kinases. *FEBS Lett.* 490:142–152. http://dx.doi.org/10.1016/S0014-5793(01)02117-2

Webber, E., L. Li, and L.S. Chin. 2008. Hypertonia-associated protein Trak1 is a novel regulator of endosome-to-lysosome trafficking. *J. Mol. Biol.* 382:638–651. http://dx.doi.org/10.1016/j.jmb.2008.07.045

Wegner, C.S., L.M. Rodahl, and H. Stenmark. 2011. ESCRT proteins and cell signalling. *Traffic*. 12:1291–1297. http://dx.doi.org/10.1111/j.1600-0854.2011.01210.x

Xu, T.R., R.F. Lu, D. Romano, A. Pitt, M.D. Houslay, G. Milligan, and W. Kolch. 2012. Eukaryotic translation initiation factor 3, subunit a, regulates the extracellular signal-regulated kinase pathway. *Mol. Cell. Biol.* 32:88–95. http://dx.doi.org/10.1128/MCB.05770-11